NANOSTRUCTURES CONSTRUCTED VIA SELF-ASSEMBLY OF NANOPARTICLES USING DNA HYBRIDIZATION

by

Kemal Oğuz Keseroğlu

Submitted to the Institute of Graduate Studies in
Science and Engineering in partial fulfillment of
the requirements for the degree of
Master of Science
in
Biotechnology

Yeditepe University
2010

NANOSTRUCTURES CONSTRUCTED VIA SELF-ASSEMBLY OF NANOPARTICLES USING DNA HYBRIDIZATION

APPROVED BY:

Assoc. Prof. Mustafa Culha (Supervisor) .....

Assist. Prof. Andrew Harvey .....

Assist. Prof. Seyda Bucak .....

DATE OF APPROVAL: 19.07.2010

“this thesis is dedicated to
the Peace in the world…”

ACKNOWLEDGEMENTS

I sincerely acknowledge The Scientific and Technological Research Council of Turkey (TUBITAK) (project number 108T605) for the financial support during this study. I also acknowledge Yeditepe University for providing crucial facility for the completion of my thesis project. I wish to thank my supervisor Assoc. Prof. Dr. Mustafa Culha for his encouraging support during the experimental and writing stages of the thesis. I also would like to thank my project friends Mehmet Kahraman and Ismail Sayin for their help in the studies. I am also thankful to my all other colleagues, namely, Ertug Avci, Ilknur Sur, Mine Altunbek, Sevcan Ayaksiz, Seda Demir, Sercan Keskin, Fatma Melis Uslu, Asli Deniz Saatci, Oxana Bondar, Erkan Yucel, Ali Yasin Sonay, Ahmet Burak Caglayan, Merve Erdem, Omer Faruk Karatas, Omer Aydin, Mahmut Ozer, Deniz Cigdem Sandal, Dilek Cam and Erdinc Sezgin.

ABSTRACT

NANOSTRUCTURES CONSTRUCTED VIA SELF-ASSEMBLY OF NANOPARTICLES USING DNA HYBRIDIZATION

Nanoparticles (NPs) are used as building blocks for construction of sensors, bio-diagnostic tools and drug delivery agents. However, the biggest challenge for their use is to construct such nanoconstructions via assembly of NPs in desired geometry into two dimensional (2D) or three dimensional structures (3D). In general, there are two approaches to prepare nanostructure: top-down and bottom-up. Lithography is an example of top-down techniques which are limited in scale and have some other limitations such as hard preparation in order and expensive instruments. On the other hand, bottom-up methods, so called self-assembly, have not scale limitations because it uses the interactions biomacromolecules, for instance DNA, RNA, peptides, lipid, carbohydrates and other small molecules. Among them, DNA seems to be an ideal material for attaining complex self-assembly due to its easily expected secondary structure and well understood of hybridization properties in Watson-Crick base pairing. Likewise, DNA is easy to be modified, sequenced and can interact with other molecules to its specific site.

In this work, it is aimed to construct two different nanostructures via self-assembly of gold nanoparticles (AuNPs) by the help of DNA. In the first one, 2D nanostructure is constructed by assembling of 13 nm AuNPs on pre-designed 4x4 DNA tile origami structure in the suspension. In the second one, differently modified two 13 nm gold colloids are assembled together by adding ten different DNA linkers to construct nano cubic structures. The prepared samples are analyzed by AFM on the surface and by Zetasizer and SAXS in the suspension. Based on the principles of nanoconstruction presented in this thesis, the construction of nanostructures for the design and preparation of much complex nanostructures using the NPs as building blocks is clarified.

ÖZET

DNA HİBRİDİZASYONUNU KULLANARAK NANOPARÇACIKLARIN KENDİLİĞİNDEN BİR ARAYA GETİRİLMELERİ YOLUYLA NANOYAPILARIN İNŞA EDİLMESİ

Nanoparçacıklar, sensor, teşhis araçları ve ilaç taşıma araçlarının yapımında yapı taşları olarak kullanılırlar. Ne var ki, nanoparçacıkların kullanımlarında, onları düzenli ve istenilen bir şekilde bir araya getirerek, onlardan 2 boyutlu veya 3 boyutlu nanoyapıların inşa edilmesi büyük bir sorun teşkil etmektedir. Nanoyapı hazırlanmasında, genellikle, 2 yaklaşım vardır: yukarıdan-aşağıya ve aşağıdan-yukarıya. Litografi yukarıdan-aşağıya tekniklerinden biridir ve gerek kısıtlı ölçek kullanımı olsun, gerekse de düzenli oluşumlar yapmanın zorluğu ve pahalı cihazlar kullanmak olsun, bazı kısıtlamaları vardır. Diğer taraftan, aşağıdan-yukarıya yöntemleri veya bir başka ifadeyle kendiliğinden bir araya getirilme yöntemleri ölçek kısıtlamalarından muaftır; çünkü bu yöntemlerde, DNA, RNA, peptit, lipit, karbonhidrat ve diğer moleküller gibi biyomakromoleküllerin birbirleri arasındaki etkileşimi kullanırlar. Bunlar arasından, DNA, kolayca beklenilen ikincil yapı oluşumu ve Watson-Crick baz paylaşımındaki hibridizasyon özelliklerinin iyi anlaşılması hasebiyle, karmaşık kendiliğinden bir araya getirilmeler için ideal malzeme gibi gözükmektedir. Ayrıca, DNA kolayca istenilen şekilde modifiye edilebilir, baz dizilimi değiştirilebilir ve diğer moleküller ile özel kısımlarından bağlanabilir.

Bu çalışmada, DNA yardımıyla altın nanoparçacıkların (AuNP) kendiliğinden bir araya getirimleri yöntemiyle, iki farklı nanoyapının inşası amaçlanmıştır. Bunlardan ilkinde, iki boyutlu yapılar, 13 nm AuNP'ların önceden tasarımı yapılmış 4x4 DNA karosu origamik yapısının üzerine toplanmasıyla süspansiyon içerisinde inşa edilmiştirler. İkinci çalışmada ise, nano ölçekte kübik yapılar oluşturmak için, yüzeyleri farklı DNA'lar ile modifiye edilmiş iki 13 nm AuNP, on faklı DNA bağlacının eklenmesiyle bir araya toplanmaları sağlanmıştır. Hazırlanan yüzeydeki örnekler AFM'de bakılırken, süspansiyon içindeki örnekler Zetasizer ve SAXS cihazlarında incelenmiştir. Bu tezde sunulmuş prensipler ışığında, NP'ların yapı taşları olarak kullanımlarıyla daha karmaşık nanoyapıların tasarlanıp hazırlanarak inşa edilmeleri izah edilmiştir.

TABLE OF CONTENTS

LIST OF FIGURES

LIST OF TABLES

LIST OF SYMBOLS / ABBREVIATIONS

d.nm	diameter in nanometer scale
Hz	Hertz
kDa	kilo Dalton
kV	kilo Volt
min	minute
nm	nanometer

1D	One dimensional
AFM	Atomic Force Microscopy
AgNP	Silver nanoparticle
AuNP	Gold nanoparticle
CNT	Carbon nanotube
DNA	Deoxyribonucleic acid
DTT	Dithiothreitol
e-beam	Electron-beam
MWCO	Molecular-weight cut-off
MNP	Magnetic nanoparticle
MRI	Magnetic resonance imaging
NASA	National Aeronautics and Space Administration
NP	Nanoparticle
ODN	Oligodeoxyribonucleic acid
Or	Origami
QD	Quantum dot
RNA	Ribonucleic acid
SAXS	Small-angle X-ray Scattering
SEM	Scanning Electron Microscopy
ssDNA	Single-stranded deoxyribonucleic acid
TEM	Transmission Electron Microscopy
UV/Vis	Ultraviolet/Visible
DLS	Dynamic Light Scattering

1. INTRODUCTION

"Nano" is derived from the Greek word "νάνος", means "dwarf"; and is used as a denoting factor of 10^{-9} in the metric system. To compare how it is too small, Figure 1.1 helps us to comprehend: a human hair has ~100 μm wide, a human cell is around 10 μm, size of a bacterium is 4 μm, width of the cell membrane is 12 nm, diameter of the DNA is 2.5 nm and an atom is around 0.1 nm.

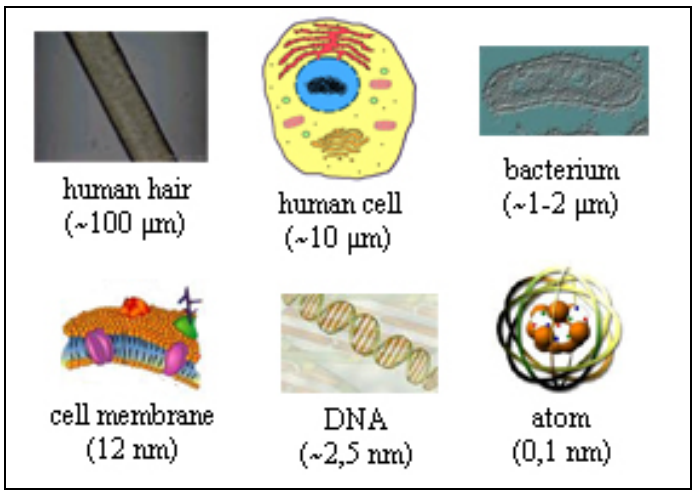

Figure 1.1. The overview of the structures from macro to nanoscale

Human beings have used nanotechnology since ancient times. Although this was an unwitting process in early times, amazing products have been made in steel, paintings and glasses such as The Lycurgus Cup from 4th century in Rome, shown in Figure 1.2. Michael Faraday realized colloidal gold which was reddish, instead of gold color, liquid contains tiny gold particles in 1857, and he first clarified that was due to the minute size of the particles [1]. After a famous talk, "There's plenty of room at the bottom", done by Richard Feynman at the California Institute of Technology on December 29, 1959, a new field of physics arose, called nanoscience [2]. He suggested that it was possible to manipulate the matter at the atomic level, however new tools had to be constructed. The development of nanotechnology was stimulated by the new techniques and vision of Professor Norio Taniguchi, first man used the term of "Nanotechnology", from Tokyo Science University in 1974 [3].

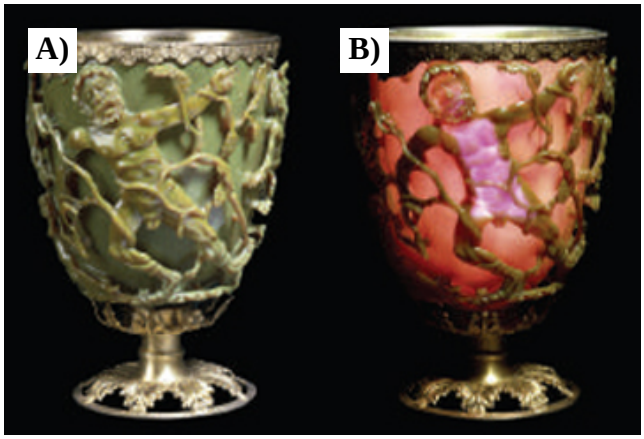

Figure 1.2. The image of the made from glass included gold nanoparticles; seen in reflected light (A) and transmitted light (B) [4]

The first definition of nanotechnology is “production technology to get the extra high accuracy and ultra fine dimensions, i.e. the preciseness and fineness on the order of 1 nm (nanometer), 10^{-9} meter in length” by Norio Taniguchi in 1974 [3]. Then it is changed to “the synthesis of novel life forms” [5]. The common definition is, today, “the technology deals with structures sized between 1 to 100 nm” [6]. However, the wide and correct one is “The creation of functional materials, devices and systems through control of matter on the nanometer length scale (1-100 nanometers), and exploitation of novel phenomena and properties (physical, chemical, biological) at that length scale” according to NASA website. “Novel phenomena and properties” is vital words in the definition due to quantum effect, otherwise it is not considered as nanotechnology.

Classical mechanics, which is also known as Newtonian mechanics, is valid in our macro life. On the contrary, as the size of the system decreases, new physical phenomena called “Quantum Mechanics” come into play. Quantum effect is dominant in the nanometer size range, and thus the physical properties of the matter are altered when compared to its similar examples in the macroscopic systems [7]. For instance, since the ratio of surface area to volume increases in nano scale; mechanical, thermal and catalytic properties of materials are changed: diffusion and reactions are faster. Additionally, opaque substances can be transparent and insoluble materials can be soluble; copper and gold, respectively [8].

In nanotechnology, there are two major bottlenecks: to synthesize nanoparticles into desired shape and size, and to assemble them into desired geometry. Even though the first problem has been overcome up to now [9-13], the latter remains as a big challenge in nano world. There are two approaches for nanoconstruction; top-down and bottom-up. Whereas top-down approaches seek to construct nanoscale devices from larger bulk materials, bottom-up approaches seek to produce them by assembling from building blocks, like as in the nature, as seen Figure 1.3. On the one hand, top-down approaches use the methods of cutting, carving and milling to shape into order for lithography. Common lithographic methods are photolithography [14], extreme UV lithography [15], electron beam lithography [16], ion beam lithography [17] and X-ray lithography [18]. Although lithography is a powerful tool, it is considered to be limited in scale [19] and have some other limitations such as difficult preparation in ordered pattern and expensive instrumentation. On the other hand, bottom-up, or so called self-assembly, approaches in nanotechnology rely on to self organize or self assemble the single nanostructures by using variety of existing forces in solution. Since it is not limited in scale, using self assembly to manufacture nanostructures is promising method in nanotechnology.

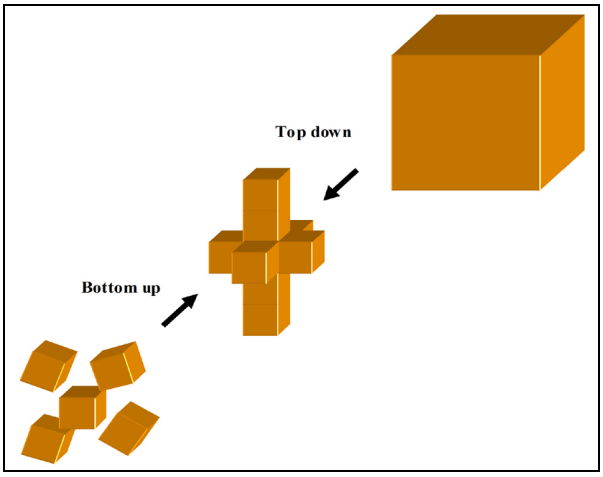

Figure 1.3. The schematic representation of top-down and bottom-up approaches for nanostructure construction

There are various applications to use constructed nanostructures and nanoparticles, such as carbon nanotube (CNT), quantum dot (QD), magnetic nanoparticle (MNP), silver nanoparticle (AgNP) and gold nanoparticle (AuNP). Figure 1.4 shows the figures that

represents some the studies for applications of these NPs. First of all, carbon nanotubes have good electrical, chemical, optical and thermal properties. CNTs can be either single wall or multi wall and their diameter can vary from 0.7 nm to 10 nm. The aspect ratio which is defined as length to diameter can be up to 10^5. There are wide application areas for CNTs in nanoelectronic devices, sensor and imaging systems, separation, purification, catalysis and energy storage [20-23]. Secondly, quantum dots are one of the milestones in nanotechnology. They have extraordinary photochemical and photophysical properties with a size range in between 1 nm to 10 nm. Depending on their size, QDs emit light in different wavelength according to their stable fluorescence capability. Common application areas of QDs are imaging systems in vivo cancer studies in medicine [24, 25]. The other group of amazing nanoparticles is magnetic nanoparticle. Since it is easy to functionalize and guide MNPs by external magnetic field, they are used in magnetic resonance imaging (MRI), catalysis, data storage and environmental remediation [26-28]. The noble metal nanoparticles, AgNPs and AuNPs, are commonly employed in many areas of science and technology due to their plasmonic properties. Since these NPs both absorb and scatter the light simultaneously, the absorbed light is effectively transferred to heat while scattered light can be used for imaging. The excitation of surface plasmons upon overlap of impinging light frequency with the oscillation frequency of electron system of the nanostructure enhances the Raman scattering, which finds variety of applications in chemistry, biology, medicine and material science [29-33]. AuNPs, however, due to their biocompatibility, they are preferably used in biomedical applications, such as in photothermal therapy [34], in gene therapy [35] and as a drug carrier [36].

The aim of this study was to investigate the assembly of AuNPs via using hybridization power of DNA. The AuNPs are chosen as model NPs due to their easy and relatively uniform size distribution. Two different nanostructures are constructed for this purpose. In the first one, the 13 nm AuNPs are assembled on pre-designed DNA origami structure in the suspension. In the second one, differently modified two 13 nm gold colloids are assembled together by adding DNA linkers to construct nano cubic structures. The prepared samples are analyzed by AFM on the surface and by UV/Vis spectroscopy, Zetasizer and SAXS in the suspension.

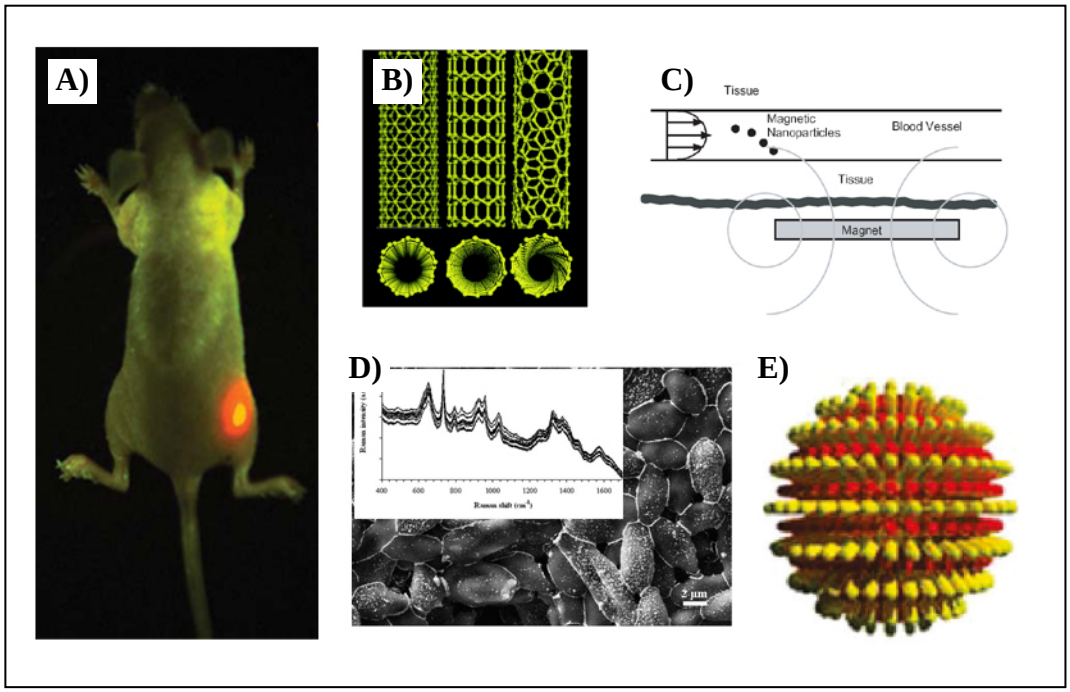

Figure 1.4. Images of QDs (A), CNTs (B), MNPs (C), AgNPs (D) and AuNPs (E) on different application areas [37-41]

2. THEORETICAL BACKGROUND

Examples of manufacturing nanostructures in the literature are briefly explained in this chapter. After top-down approaches are discussed, selected studies of self assembly are explained in detail and finally the importance of the bottom-up approach is emphasized.

2.1. TOP DOWN APPROACHES

Top down approaches start with large scale bulk materials and reduce its dimensions to form nanostructures. Most common lithographic techniques are photolithography, e-beam lithography, ion-beam lithography and X-ray lithography. Among them, photolithography, widely used one, is described in detail.

2.1.1. Photolithography

Photolithography comes from combination of Latin words “light-stone-writing”. Generally, it is the process that geometric shapes on an optical mask are transferred to the surface of a silicon wafer [42]. Before starting, the wafer first is chemically cleaned from organic, ionic and metallic impurities. Then the surface of the wafer is deposited by silicon dioxide for barrier layer. After deposition, photoresist coating is applied by spin coating. There are two types of photoresist: positive and negative photoresist. In the former one, where the UV light is exposed on, the material is removed. However, when the light is exposed to negative resist, it remains on the surface. Although negative resists were initially used in the early times, positive resists are widely used now because of better controllability for small shapes. Then the solvents from photoresist coating are removed. This process is called soft-baking which has critical role for photosensitivity of the photoresist. Finally, the mask has to be aligned before UV light exposure. The light is usually chosen at smaller wavelength; because, according to Abbe’s principle, the resolution is proportional to the wavelength and inversely to the angle of exposure. For that reason, Fluorine lasers are used in the industry. However, as the wavelength is reduced, the system becomes more complicated and the cost of the manufacturing increases.

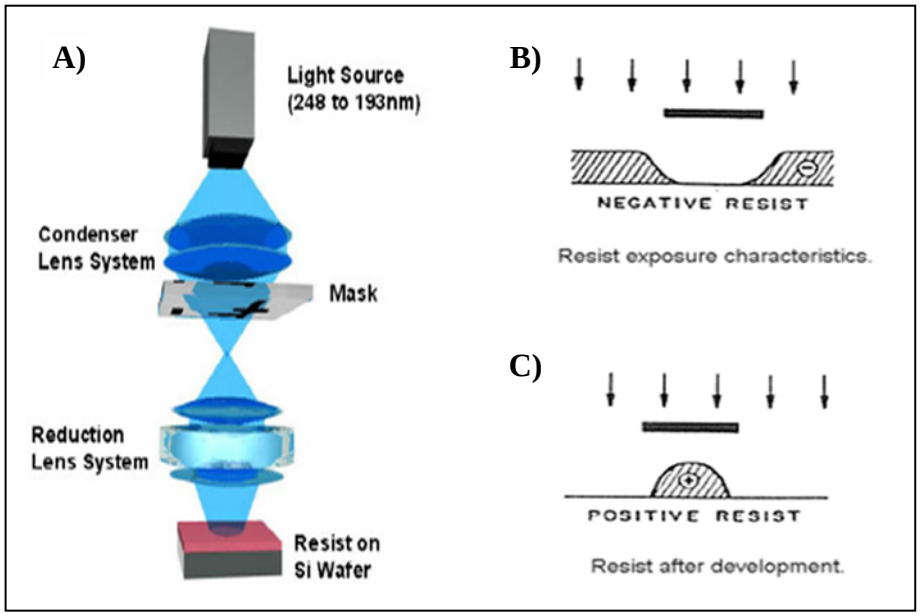

Figure 2.1. Schematic representation of photolithography (A) and negative (B) and positive resists (B) [42]

2.1.2. Other Lithographic Techniques

One of the other lithographic techniques is e-beam lithography. Since the wavelength of an electron beam is shorter than the light, e-beam lithography has been used for many years instead photolithography. In order to direct the electron beam, magnetic lenses are used, in place of condenser lenses in photolithography. Although the spot size is very small as 0.5 nm, the resolution of the system is limited by the scattering distance of the electrons. The main problem of the e-beam lithography is, however, slow process to manufacture. As for ion-beam lithography, ionized atoms are used in this system. Being heavier of ionized atoms than electrons provides it to be more convenient to control them by lenses. Additionally, heavy ions scatter less than electrons. On the other hand, the ion-beam lithography is still slow process like as the previous ones. Finally, X-ray lithography is used in the industry. It is based on the X-rays as an exposure source. Therefore, X-ray lithography is extremely expensive due to the fact that it is difficult to obtain high quality X-rays [42].

All in all, top-down approaches have to be replaced with bottom-up approaches in order to construct high throughput, less expensive nanostructures.

2.2. BOTTOM UP APPROACHES

Bottom up, or self assembly, approaches are the rising sun of nanofabrication. Although it is most similar to the behavior in the nature and a more promising approach compared to top-down, it still has to be developed. In this part of the chapter, self assembly is discussed in two sections: self assembly at liquid-liquid interface and self assembly at solid-liquid interface.

2.2.1. Self Assembly at Liquid-Liquid Interfaces

Liquid-liquid interfaces are used in the organization of nanoscale objects. It is possible to produce defect-free nanosurfaces [43] by using the interface of two immiscible liquids such as oil-water interface where the interfacial tension is high [44]. In one example, CdSe nanoparticles are assembled at water-chloroform interface [45]. In another one, heterodimeric nanoparticles are formed by subsequent seeding of AgNPs on the outside of assembled Fe_3O_4 nanoparticles on a liquid-liquid interface [46]. The self assembly of NPs at liquid-liquid interfaces stems from the decreasing of high interfacial energy between two liquids by assembly of NPs at the interface [47].

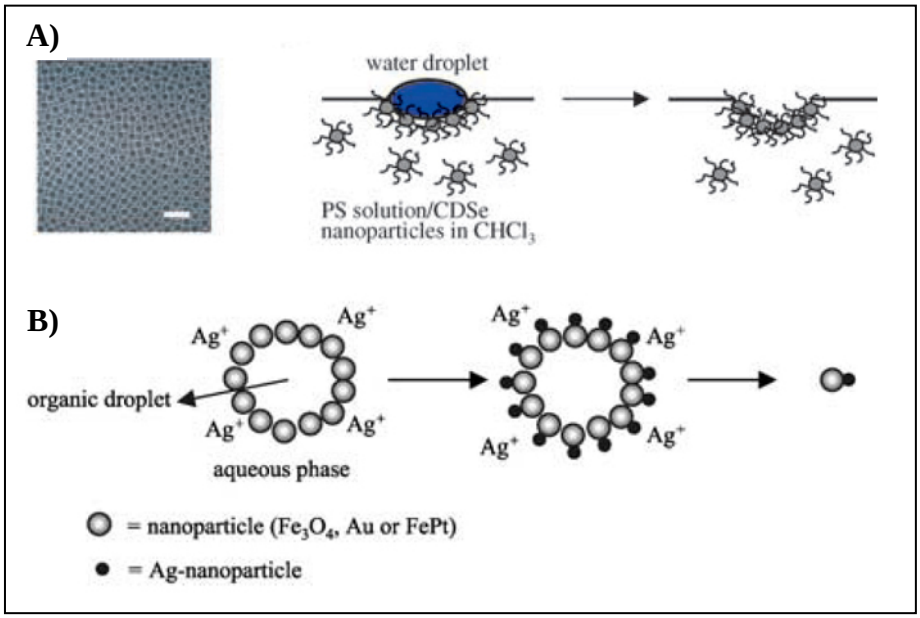

Figure 2.2. Assembly of CdSe NPs at water-chloroform interface [45] (A) and formation of heterodimeric NPs at liquid-liquid interface [46] (B)

2.2.2. Self Assembly at Solid-Liquid Interfaces

The self assembly of NPs can be achieved at solid-liquid interfaces. Basically, this approach includes to assemble the NPs from their suspensions to solid surfaces into one dimensional (1D), 2D and 3D structures. In this technique, supramolecular interactions (for instance: electrostatic interactions [48], oligonucleotides [49], metal complexes [50], directed hydrogen bonds [51] and hydrophobic forces [52]) between surface and NPs are used. This type of self assembly can be considered in three different parts as in drying droplet, template assisted and programmed self assembly.

2.2.2.1. Self Assembly from a Drying Droplet

As the droplet dries, there is a pattern remaining on the surface. The controlling distribution of the NPs in a drying droplet of suspension placed on surfaces has critical importance for the assembly of the NPs prepared in suspensions. For this reason, several studies have been reported for 20 years [53-57]. When a droplet is placed onto the surface, it pins from the contact line at the surface depending on the roughness of the surface, a phenomenon known as “contact line pinning” [56, 57]. While evaporation, in order to keep the contact line fixed, it is replenished by the liquid from the interior part which causes not only to evaporate faster at the edges, but also to form a ring at the perimeter of the droplet. This replenishment process drags all particles to the pinned contact line and piles them up to form a ring-like structure, known as “coffee ring”. Nevertheless, several studies investigated in details for the assembly of the NPs in drying droplet, even in a moving droplet [58]; it is still needed to understand to control the assembly of NPs in a sessile droplet. The complexity of the process requires further investigation to control the behavior of the NPs to benefit from the process to assemble the NPs.

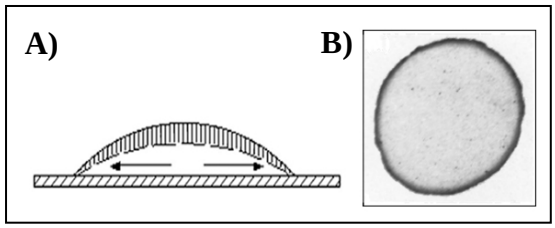

Figure 2.3. Outward flow mechanism of the drying droplet pinned from contact line (A) and image of a dried droplet (B) [56]

2.2.2.2. Template Assisted Self Assembly

In this approach, self assembly can be directed on a template that is often fabricated by top-down approaches, such as e-beam lithography and light lithography or chemical applications such as co-polymer and chemical functionalization [59]. For example, in the study of Cui et al., 50 nm gold nanoparticles are assembled into the wells that are defined by electron-beam lithography as seen in Figure 2.4 [60]. For directing NPs, surface topography, electric and magnetic fields or shear forces can be used. Even supramolecules [61] and particles [62] can be used as template.

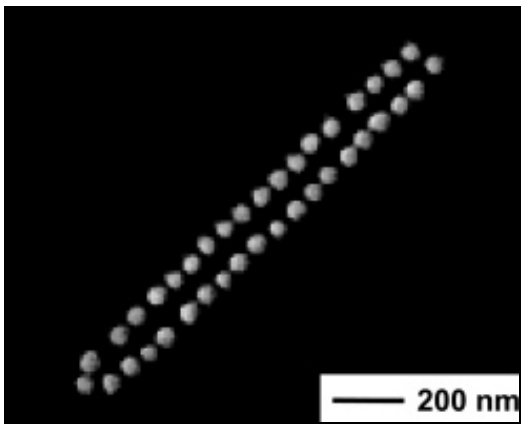

Figure 2.4. SEM image of 50 nm AuNPs assembled into wells defined by e-beam lithography [60]

2.2.2.3. Programmed Self Assembly

Programmed self assembly is another key approach to build nanostructures and nanodevices. Although current ability to form nanoconstructs is quite limited compared to lithographic techniques, it is the most promising technique due to the absence of scale limitation and being high throughput construction contrary to top-down approaches. In programmed self assembly, the interaction between natural molecules for instance DNA [63], RNA [64], peptide [65], lipid [66], carbohydrates [67] and other small molecules [68], are used to construct nanostructures. Among them, DNA seems to be an ideal material for attaining complex self-assembly due to its easily expected secondary structure and well understood hybridization properties in Watson-Crick base pairing. Likewise, DNA is easy to be modified and can interact with other molecules on its specific site. Additionally, structures made of DNA can be easily designed by computer.

In this section, some of the fundamental examples of programmed self assembly of NPs by DNA from the literature are summarized. In the first study of Mirkin et al., oligodeoxynucleotide (ODN) bound 13 nm AuNPs are assembled by the hybridization of ODNs with the linker DNA strands [69] in 1996. Then, Mucic et al. showed the production of 2D shape from the assembly of AuNPs by combination of small sized NPs (8 nm) on a large one (31 nm) by using DNA hybridization between ssDNAs on the NPs [70]. Meanwhile, Alivisatos et al. investigated the organization of ODN-bound AuNPs by hybridization on a ssDNA molecule [71]. With this study, it was shown that it is possible to arrange NPs on a DNA molecule to form larger nanostructures. However the final DNA molecule was very simple for the complex structures, it was linear and the NPs can only be arranged along that line. Afterwards, new strategies were developed to produce complex and more rigid structures from DNA, called DNA Origami [72, 73]. In this strategy, large DNA structures are engineered by folding of a single stranded long ODN with smaller DNA strands, staple strands. For the backbone strand, a circular single stranded viral genome, M13 bacteriophage, is generally used and staple strands vary in length, up to 30 base pairs (bp). By using DNA Origami, it becomes possible to produce 2D DNA shapes; such as star, smiley faces and triangles, as shown in Figure 2.5. In 2003, the group of LaBean and Yan designed 4x4 DNA tiles from DNA Origami and made 2D grids by assembling the tiles [74]. Seaming of DNA Origami is also possible which provides to produce 3D shapes from DNA. Last years, Andersen et al. made a 3D DNA box with a controllable lid [75] and Sharma et al. made DNA tubules [76].

As a novel idea, different from the literature, in the first part of the thesis, a nanostructure is aimed to construct by attaching of ODN-bound AuNPs on to the free parts of 4x4 DNA Origami which is inspired by the study of Yan.

In another approach, DNA nanotechnology deals with the crystallization of DNA-directed colloids [77-80]. Firstly, in 2008, Nykypanchuk et al. investigated the organization of AuNPs aggregation by using DNA hybridization through a heating-cooling cycle [77]. The AuNPs were assembled from the hybridization of their ODNs that bind to their surface with variety of spacer lengths from the NP side. Formation of crystalline structures was observed from SAXS analysis. At the same times, the group of Mirkin showed that body-centered cubic and face-centered cubic crystal structures were possible

to be directed by the absence or presence of a non-bonding single base flexor which was located at both sides of the hybridized part which is in the middle [78].

In the second part of this thesis, AuNPs are functionalized with two different ODNs separately, while one type of ODNs binds from 5’ end, the other binds from 3’ end. The purpose is to aggregate AuNPs in a controlled way by adding a DNA linker which has complement sequences with both ODNs and 0 to 9 unpaired bases. The controllable aggregation of the NPs by a DNA linker addition and the effect of unpaired bases between the hybridized strands are investigated.

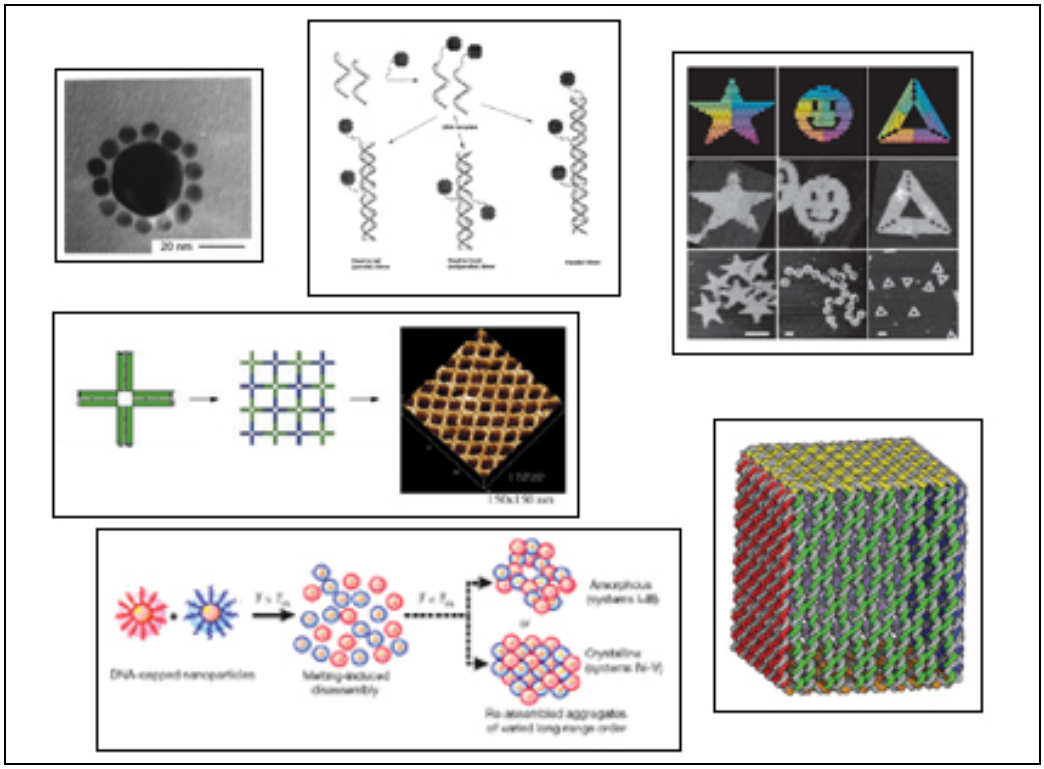

Figure 2.5. Images selected from fundamental studies in DNA nanotechnology [70, 71, 73-75, 77]

3. MATERIALS

3.1. REAGENTS

$HAuCl_4.3H_2O$ was purchased from Fluka (Taufkirchen, Germany) and sodium citrate was purchased from Merck (New Jersey, USA) for synthesis of gold nanoparticles. The oligodeoxynucleotides (ODNs) were purchased from Invitrogen (California, USA) and AlphaDNA (Quebec, Canada) as shown in Table 3.1 and Table 3.2. Dithiothreitol (DTT) was purchased from Bio Basic Inc. (New York, USA) for deprotection of dithiolated ODNs and PCR purification kit from Promega (Wisconsin, USA). Finally, 10K MWCO Slide-A-Lyzer Dialysis Cassettes were purchased from Thermo Fisher Scientific Inc. (Illinois, USA).

3.2. OLIGODEOXYNUCLEOTIDES (ODNs)

The ODNs were purchased as 200 nmol (desalted) and prepared as 100 μM with dH_2O. Table 3.1 and 3.2 show the sequences of the ODNs to be used in two different studies: constructing nanostructures by using DNA Origami and constructing nanostructures by adding DNA linker, respectively. D1, D2, D14 and D15 are thiol modified ODNs; while D1 and D14 are modified from 5’ end and unprotected, D2 and D15 are modified from 3’ end and protected which means have not got free –SH at the end. The remains are single-stranded DNA (ssDNA) molecules. The sequences are given as from 5’ end to 3’end.

Table 3.1. The properties of ODNs used in constructing nanostructures by using DNA Origami

Label	Sequence (from 5’ to 3’)	Base number	Brand
D1	HS-$(CH_2)_6$-TTTTTTTTTTTTTTTTTTT	20	Alpha DNA
D2	TTTTTTTTTTTTTTTTTTTT-$(CH_2)_6$-S-S-$(CH_2)_5$-CH_3	20	Alpha DNA
D3	AGGCACCATCGTAGGAAAATCTGCGTCAGCTCT CCGTACACCAGTGCTTCCATGCGAAGTAAAAC GTTCCGATCACCAACGGAGTAAAACGATCTAA CTGATAACTAGCACCTCTGCTCACGTGAGGAGT AAAACTTGCC	140	Alpha DNA
D4	ATACCGGAGGCTTCCTGTACGGAGAGCTGACG CAGACCTACGATGGACACGCCG	54	Invitrogen
D5	ATGCAACCTGCCTGGCAAGACTCCTCACGTGAG CAGAGGACTACTCATCCGTTA	54	Invitrogen
D6	TTTCCGACTGAGCCCTGCTAGTTATCAGTTAGA TCGACTCCGTTGGACGAACAG	54	Invitrogen
D7	ATAGCGCCTGATCGGAACGACTTCGCATGGAA GCACTGGACCGTTCTACCGATT	54	Invitrogen
D8	CTCGCAATCGGTAGAACGGTGGAAGCCTCCGG TATGCATG	40	Invitrogen
D9	AAAAAAAAAACGGCGTGTGGTTGCATAAAAAA AAAA	36	Invitrogen
D10	CGCTATAACGGATGAGTAGTGGGCTCAGTCGG AAAAGGTC	40	Invitrogen
D11	AAAAAAAAAACTGTTCGTGGCGCTATAAAAAA AAAA	36	Invitrogen
D12	TAGCGAATCGGTAGAACGGTGGAAGCCTCCGG TATGACCT	40	Invitrogen
D13	GCGAGTAACGGATGAGTAGTGGGCTCAGTCGG AAACATGC	40	Invitrogen

Table 3.2. The properties of ODNs used in Constructing Nanostructures by adding DNA Linker

Label	Sequence (from 5’ to 3’)	Base number	Brand
D14	HS-$(CH_2)_6$-AAAAAAAAAAATGTGTGGAGTTGGCTGTTACGACTA	36	Alpha DNA
D15	CTCAGCCCAGGTTCAGTTCTGGTCATAAAAAAAAAA-$(CH_2)_6$-S-S-$(CH_2)_5$-CH_3	36	Alpha DNA
D16	ATGACCAGAACTGAACCTGGGCTGAGTAGTCGTAACAGCCAACTCCACACAT	52	Invitrogen
D17	ATGACCAGAACTGAACCTGGGCTGAGATAGTCGTAACAGCCAACTCCACACAT	53	Invitrogen
D18	ATGACCAGAACTGAACCTGGGCTGAGAATAGTCGTAACAGCCAACTCCACACAT	54	Invitrogen
D19	ATGACCAGAACTGAACCTGGGCTGAGAAATAGTCGTAACAGCCAACTCCACACAT	55	Invitrogen
D20	ATGACCAGAACTGAACCTGGGCTGAGAAAATAGTCGTAACAGCCAACTCCACACAT	56	Invitrogen
D21	ATGACCAGAACTGAACCTGGGCTGAGAAAAATAGTCGTAACAGCCAACTCCACACAT	57	Invitrogen
D22	ATGACCAGAACTGAACCTGGGCTGAGAAAAAATAGTCGTAACAGCCAACTCCACACAT	58	Invitrogen
D23	ATGACCAGAACTGAACCTGGGCTGAGAAAAAAATAGTCGTAACAGCCAACTCCACACAT	59	Invitrogen
D24	ATGACCAGAACTGAACCTGGGCTGAGAAAAAAAATAGTCGTAACAGCCAACTCCACACAT	60	Invitrogen
D25	ATGACCAGAACTGAACCTGGGCTGAGAAAAAAAAATAGTCGTAACAGCCAACTCCACACAT	61	Invitrogen

4. METHODS

4.1. SYNTHESIS OF GOLD NANOPARTICLES

13 nm size of spherical AuNPs were synthesized using the citrate reduction method [13]. Firstly, 0.2-g of $HAuCl_4.3H_2O$ was dissolved in 500 ml distilled water in an Erlenmeyer flask well cleaned by chromic acid. This solution was heated and stirred until boiling. After boiling, 50-ml of 38.8 µM sodium citrate was added slowly. The solution was kept boiling for 15 min. After cooling, the colloidal suspensions were filtered by 0.45 µm filter. Figure 4.1 shows the UV/Vis spectroscopic analysis and the image of the suspension. Maximum absorption is measured at 520 nm. Average size distribution by number of the colloidal suspension is measured as 13 nm in Zetasizer and shown in Figure 4.2 which is consistent with the TEM image of spherical AuNPs shown in Figure 4.3.

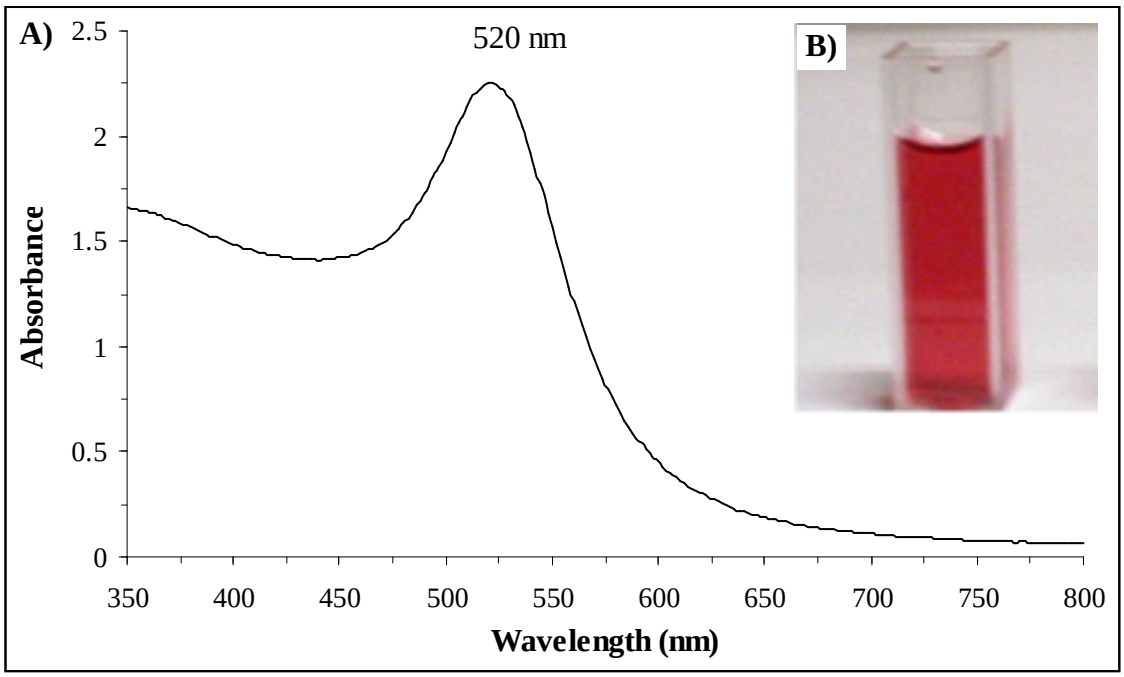

Figure 4.1. UV-Vis spectroscopic characterization of 13 nm AuNPs

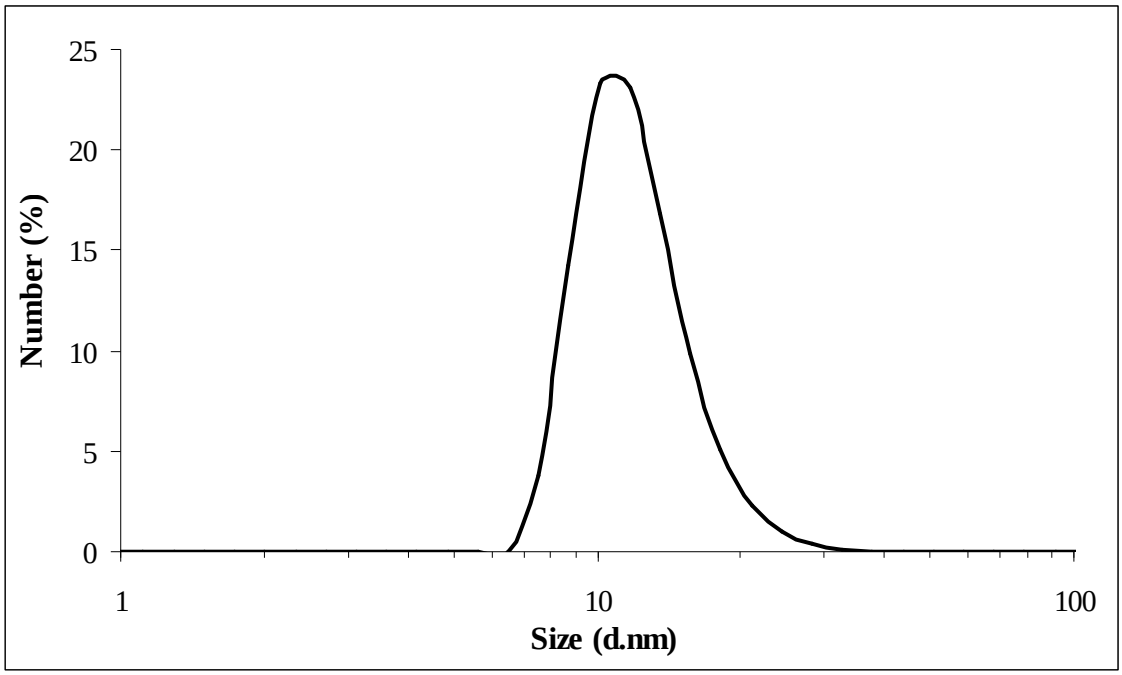

Figure 4.2. Zetasizer size distributions by number of synthesized colloidal gold suspension

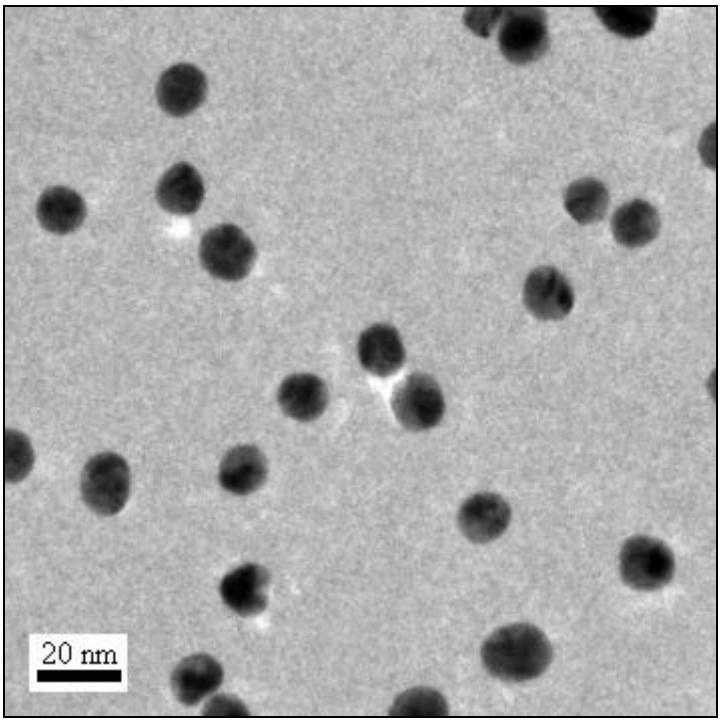

Figure 4.3. TEM image of 13 nm AuNPs

4.2. DEPROTECTION OF THIOLATED ODNs

Since D2 and D15 were purchased as protected, their moiety needs to be deprotected, which means to break S-S bond attached to the $-(CH_2)_5CH_3$ and make the 3' end of ODN as free thiol bond (-SH). For this purpose, D2 and D15 ODNs were incubated in 0.1 M dithiothreitol (DTT) at 55 ^oC for 16 hours. DTT is a reducing agent that cleaves the disulfide bond of a molecule. The excess molecules were removed from the solution by purification kit.

4.3. BINDING OF THIOLATED ODNs TO GOLD COLLOIDS

The synthesized AuNPs possess citrate ions on their surfaces. Replacing of citrate ion with thiol of the modified ODN makes ODN possible to bind chemically on the gold colloid. According to Hill et al, the capacity for loading of a 13 nm AuNP with ODN is 110 ODN per particle [81]. The concentration of synthesized gold colloid suspension is 10^{12} AuNPs per ml [13]. Therefore, in order to load fully each AuNP with thiol modified ODNs, higher than 10^{14} ODNs were added to 1-ml of colloidal suspension. To increase binding kinetics, the suspension was shaken over night.

4.4. DIALYSIS OF ODN BOUND AuNP SUSPENSION

Although it is supposed that all ODNs are bound to the surface of AuNPs, some of them might be not. Consequently, unbound ODNs, also the excess citrate, were removed from the suspension by using 10,000 MWCO Slide-A-Lyzer Dialysis Cassettes. The membranes of the cassettes only allow the passage of molecules below a certain molecular weight (MW), 10KDa. Since MW of 13 nm AuNP is much higher than 10 KDa and that of all used ODN molecules and citrate ions are less, the remaining solution would be only have ODN-bound 13 nm AuNPs. After the cassettes were loaded with the suspensions, they are placed in a beaker containing 2 liter distilled water. The water was changed 3 times every 2 hours and finally the beaker was kept at 4 ^oC in a refrigerator over night. The suspension was taken in and out by a syringe. Figure 4.4 shows the Zetasizer analysis before and after dialysis of D1-bound AuNP suspension and it is clearly seen that unwanted molecules are removed and the average size of particle increased to 15 nm.

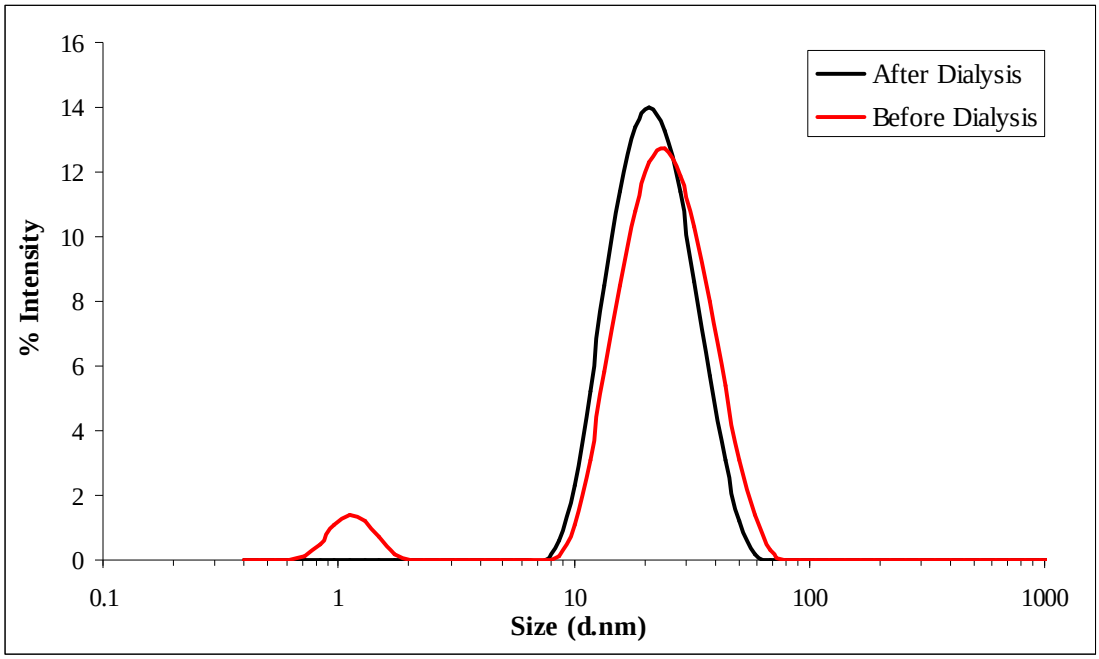

Figure 4.4. Zetasizer size distributions of D1 bound 13 nm AuNP before and after dialysis

4.5. CONSTRUCTION OF NANOSTRUCTURES

4.5.1. Constructing Nanostructures by Using DNA Origami

4.5.1.1. Constructing DNA Origami

Two DNA Origami were produced by combining of certain ODNs as shown in Table 4.1 and labeled as Origami-A (OrA) and Origami-B (OrB). The differences between the Origami are the sticky ends that are labeled in color as shown in Figure 4.5 and Figure 4.6. While producing Origami, the DNA mixture was run in 1% agarose gel once to observe controlled hybridization. The final concentration of the Origami was 1 μM. The reason for using two Origami is to control the elongation of the Origami structure. The elongation achieved by hybridizing from sticky ends.

Table 4.1. The ODNs list to construct Origami-A and Origami-B in order

Origami-A	D3+D4+D9+D5+D10+D6+D11+D7+D8
Origami-B	D3+D4+D9+D5+D13+D6+D11+D7+D12

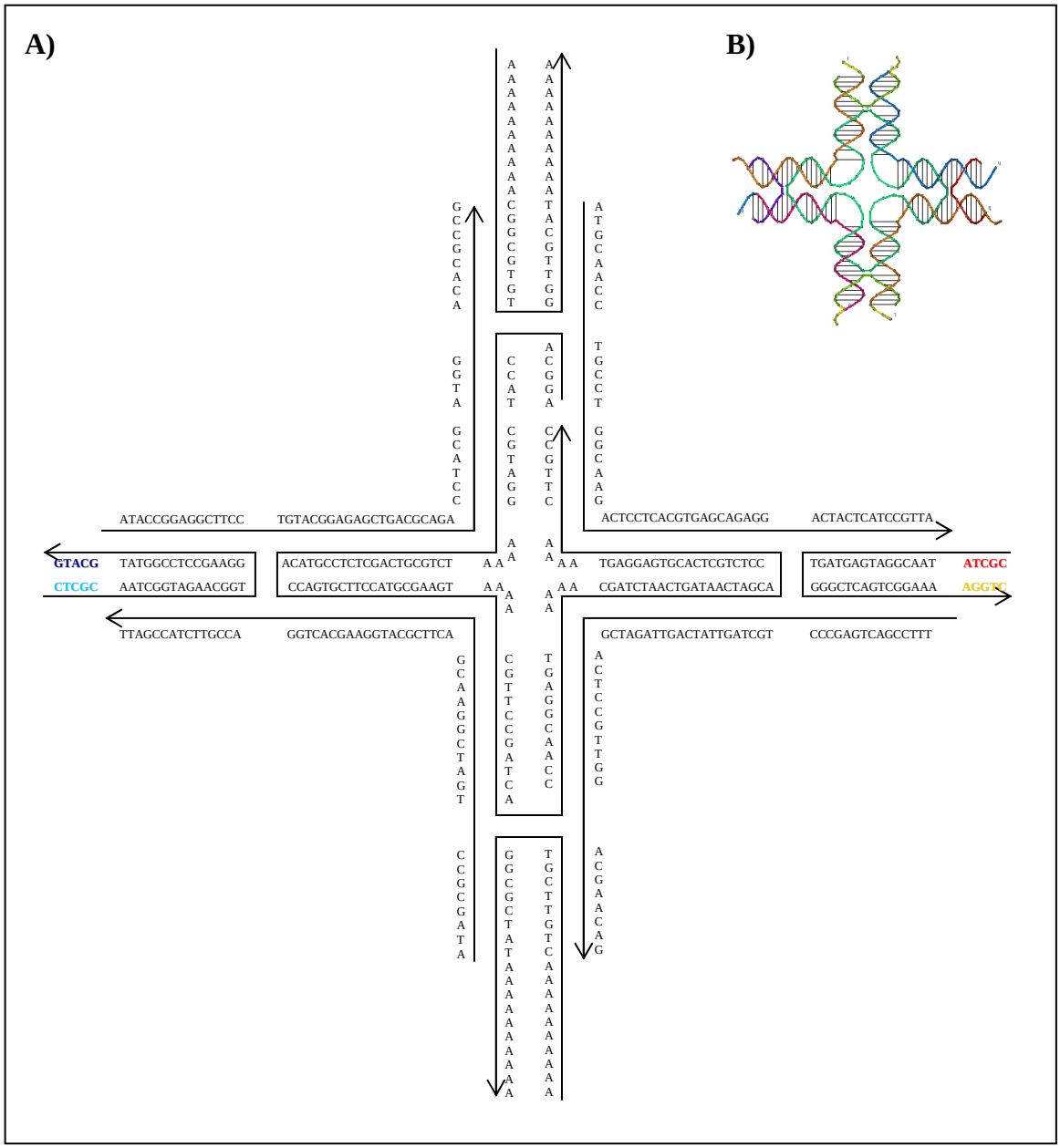

Figure 4.5. Design of Origami-A with sequences (A) and its schematic representation (B)

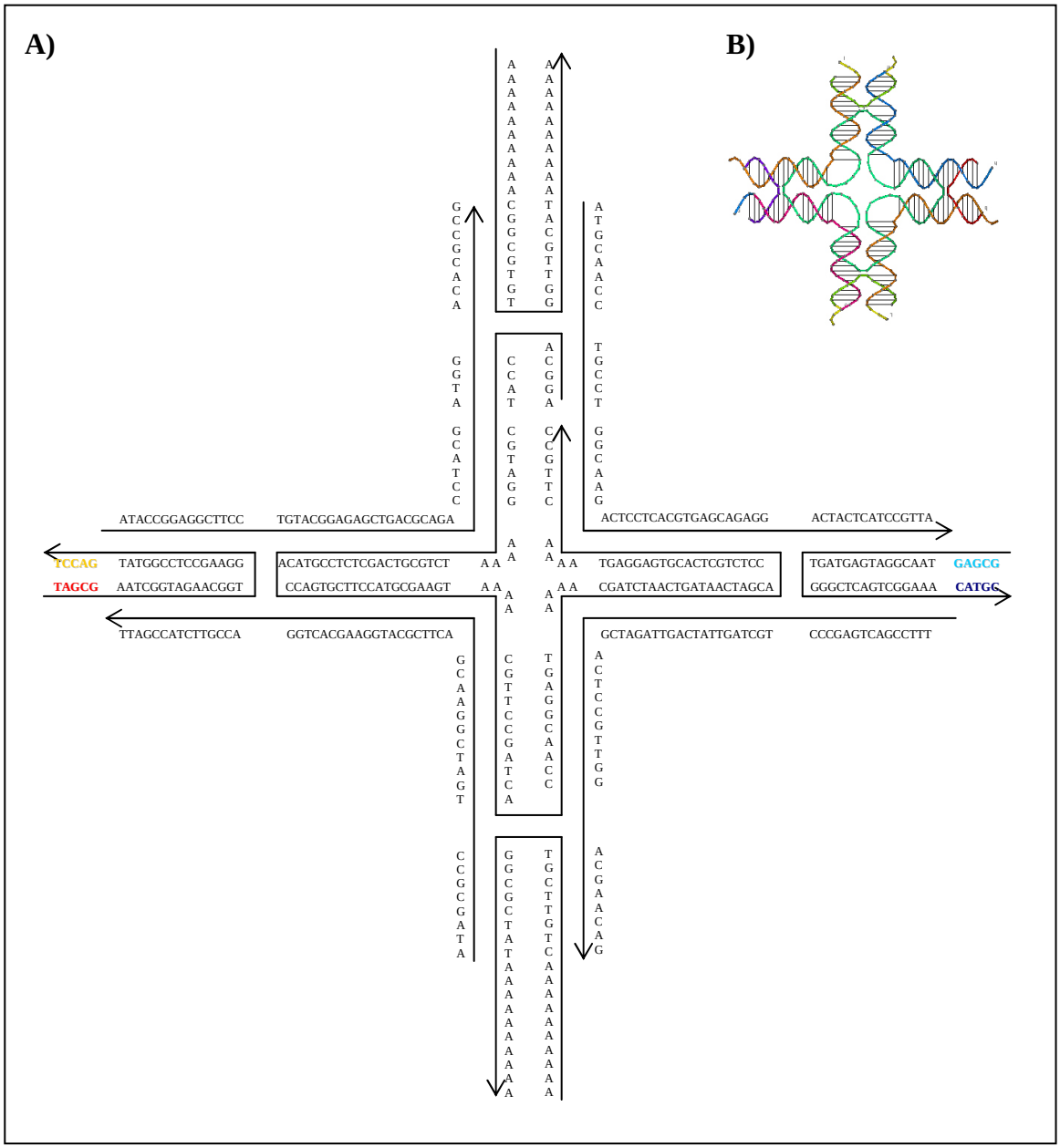

Figure 4.6. Design of Origami-B with sequences (A) and its schematic representation (B)

4.5.1.2. Binding of ODN-Bound AuNPs to Constructed DNA Origami

D1-bound 13 nm AuNPs and D2-bound 13 nm AuNPs were attached to Origami-A and Origami-B separately, as seen in Figure 4.7. Additionally, Figure 4.8 shows the ODN-bound AuNPs were attached to OrA and OrB mixture. The constructed structures were analyzed under AFM.

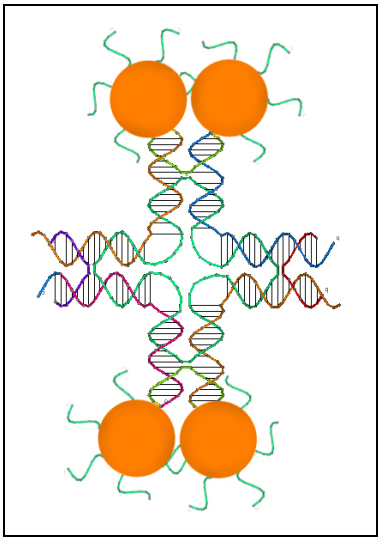

Figure 4.7. Schematic representation of DNA Origami attached to ODN-bound AuNPs

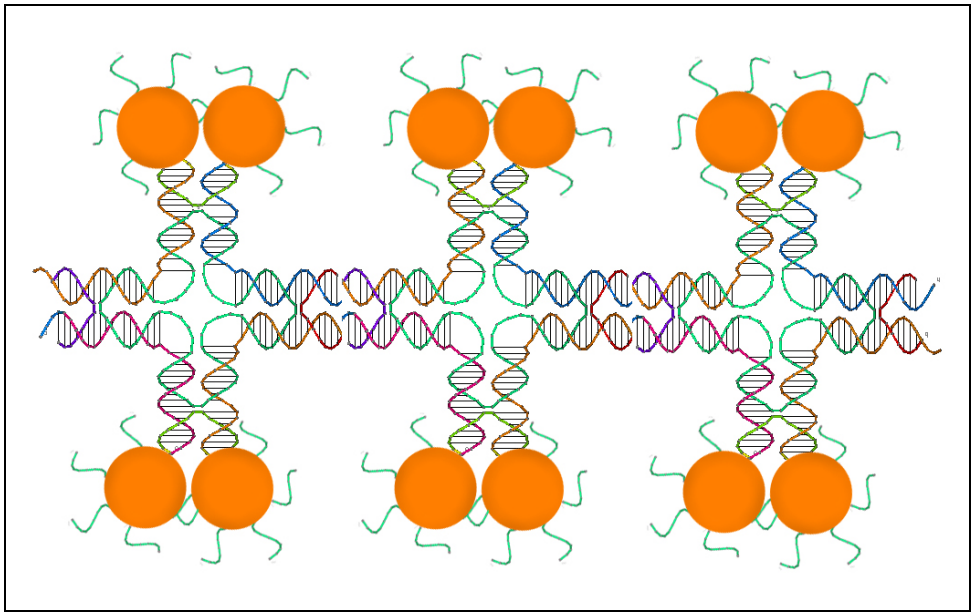

Figure 4.8. Schematic representation of hybridized Origami-A and Origami-B attached to ODN-bound AuNPs

4.5.2. Constructing Nanostructures by Adding DNA Linker

Another independent study of the thesis includes constructing nanostructures, especially cubic structures in nano scale, by adding DNA linkers to ODN-bound AuNPs. For this purpose, 13 nm AuNPs were bound with D14 and D15 individually. Then, ten different DNA linkers were added to a mixture of D14-bound and D15-bound AuNPs. As seen Figure 4.9, the DNA linkers have complementary sequences to D14 and D15. While D16 hybridized from its all sequences, D25 has nine spacer bases. Table 4.2 shows the variation of the sequences for each DNA linker. The constructed structures were analyzed with Zetasizer and UV-Vis spectroscopy to observe growth of the construction and SAXS to observe the crystal form of nanocubic structure.

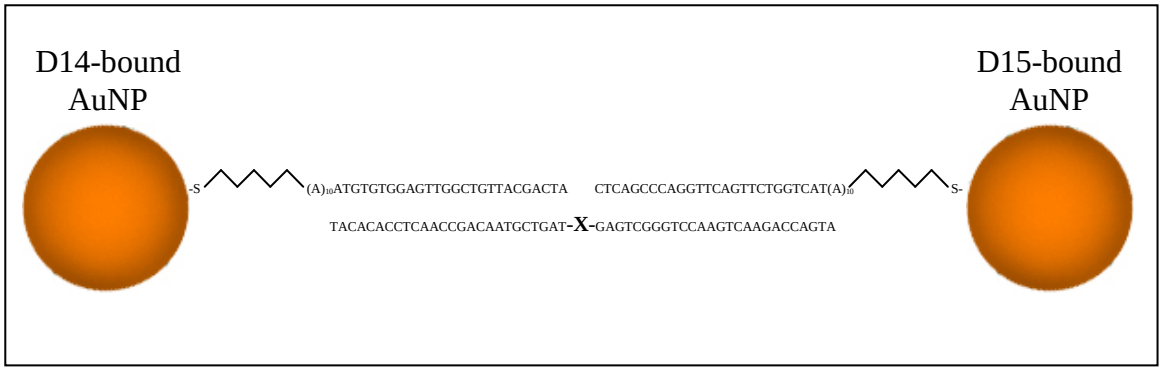

Figure 4.9. Schematic representation of how the DNA linker assembles the two different ODN-bound 13 nm AuNPs

Table 4.2. Sequence variation at the middle position for each DNA linker

Label	Sequence of X
D16	
D17	A
D18	AA
D19	AAA
D20	AAAA
D21	AAAAA
D22	AAAAAA
D23	AAAAAAA
D24	AAAAAAAA
D25	AAAAAAAAA

4.5.3. Dynamic Light Scattering Analysis

Dynamic Light Scattering (DLS) measurements were performed using a Zetasizer nano-ZS from Malvern Instruments (Malvern, UK). Each sample was measured three times and average size was determined by number for synthesized nanoparticles and by intensity for measurements of constructions by adding DNA linkers.

4.5.4. Atomic Force Microscopy Analysis

The AFM analyses were performed with a Park SYSTEMS XE 100 Atomic Force Microscopy (Park Systems Corp. KANC 4F, Iui-Dong, 906-10 Suwon 443-766, Korea). Imaging was carried out at room temperature in non-contact mode with silicium tips with varying resonance frequencies at a linear scanning rate of 0.5, 1 or 1.5 Hz.

4.5.5. Transmission Electron Microscopy Analysis

TEM measurements were performed on JEOL-2100 HRTEM operating at 120 kV and 200 kV (LaB_6 filament) and equipped with an Oxford Instruments 6498 EDS system. Copper TEM grids coated with carbon support film were used to analyze samples upon placing very small drops of samples onto them.

4.5.6. Small Angle X-Ray Scattering Analysis

SAXS analysis were carried out by Hecus-SWAXS systems (Graz, Austria) with a linear-position-sensitive detector (MBraun, Garching, Germany) containing 1024 channels. CuKα radiation (λ=1.54 Å) which was produced by an X-ray generator operating at 50 kV and 40 mA (Philips, PW 1830/40, The Netherlands) was used. The sample was placed in a capillary tube with 1 mm thickness for analysis. The sample to detector distance was 268 mm and the exposure time was 700 sec per sample. MATCAL, EASY SWAXS and 3D-View software were used in data analysis.

5. RESULTS AND DISCUSSION

5.1. CONSTRUCTING NANOSTRUCTURES BY USING DNA ORIGAMI

5.1.1. Electrophoresis Gel Analysis

DNA Origami is a well defined and rigid structure compared to other DNA structures. Since it has more than one intersected double helices, we need to be sure all ODNs are hybridized with each other. In order to observe this, the DNA mixtures were loaded in a 2% agarose gel and run at 100 V for 30 min. 100 bp ladder was used as a marker. The gel photo is seen in the Figure 5.1. While the second well contains only D3, the third one was loaded D3 and D4 mixture. The next one contains D3, D4 and D9. The others were loaded with the addition of next ODN to previous mixture. The ninth well has the Origami-A. As seen in Figure 5.1, all ODNs are hybridized with the previous mixtures understood from getting heavy each time and not seeing any unhybridized ODN.

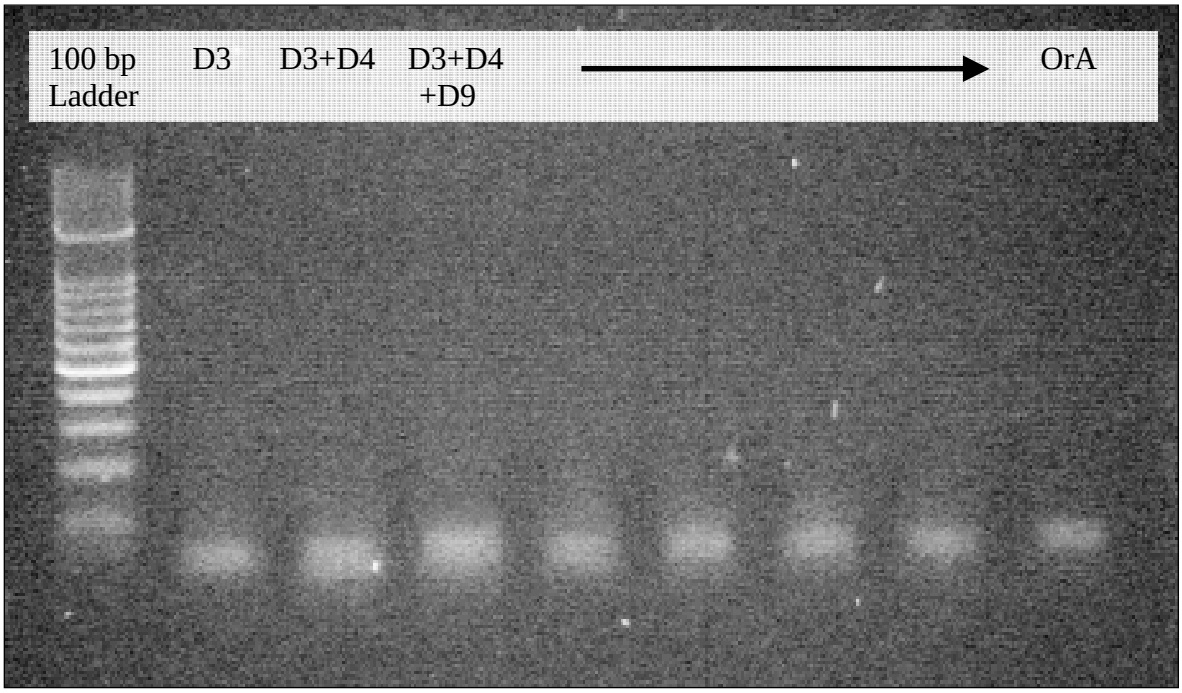

Figure 5.1. Photo of 2% Agarose gel loaded with ODNs for each step while construction of DNA Origami

5.1.2. Atomic Force Microscopy Analysis

5.1.2.1. Origami-A and Origami-B

After Origami-A or Origami-B was constructed, they were observed under AFM, Figure 5.2. AFM line analysis reveals the dimension to be approximately 4 nm height and 40 nm width which corresponds to the expected dimensions of the DNA Origami. As DNA Origami is not as rigid as a metal, AFM only gives a general outline of the constructed DNA Origami. The width of the sample is measured to be larger from the expected value, 30 nm, possibly due to low resolution scanning of the AFM tip. The height, on the other hand, gives generally more accurate information about the sample, and is close to the expected range or 2.5-5 nm.

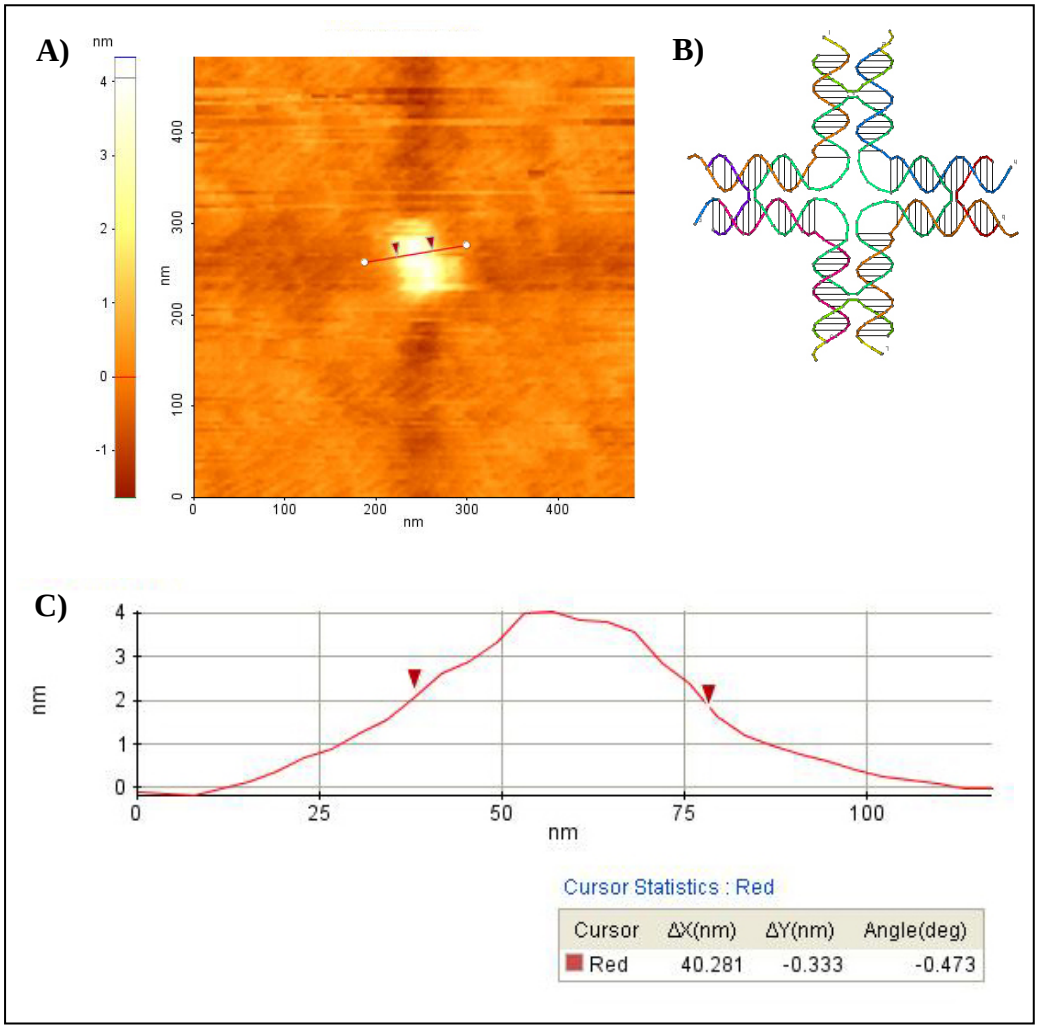

Figure 5.2. AFM image (A), schematic representation (B) and line analysis (C) of Or-A

5.1.2.2. Mixture of Origami-A and Origami-B

The mixture of Origami-A and Origami-B is also important for further constructions. Figure 5.3 shows they were hybridized from sticky ends as previously described in Figure 4.5 and 4.6. The line analysis shows us that it has around 4 nm height and 30 nm width, similar to the Origami-A or B alone. However, the length is more than 100 nm which suggests at least 3 Origami are hybridized end to end.

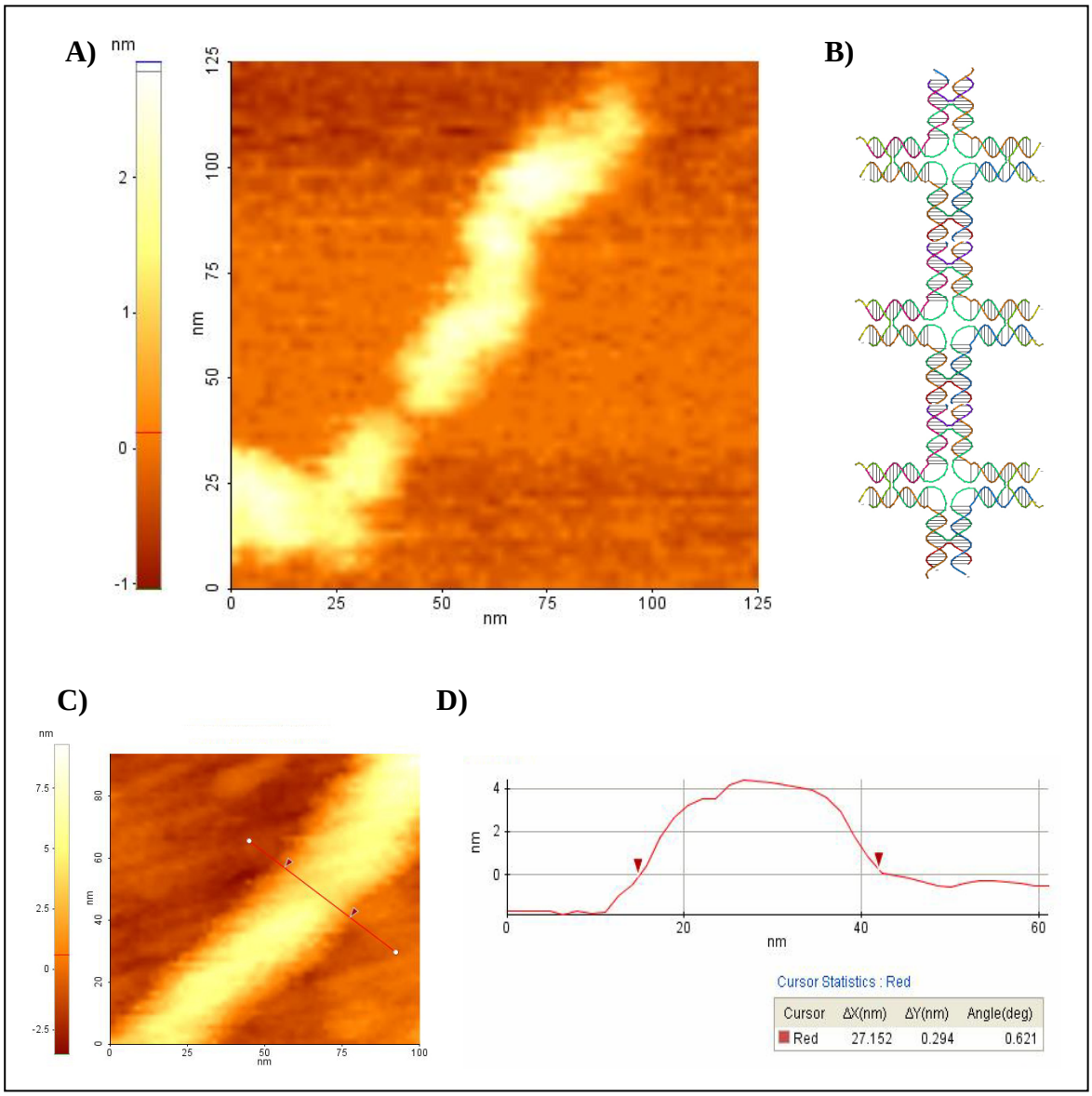

Figure 5.3. AFM images (A, C), schematic representation (B) and line analysis (D) of Origami-A and Origami-B mixture

5.1.2.3. D1-Bound AuNPs Attached to Origami-A

Another important step is attaching of AuNPs to the DNA Origami. For this purpose, firstly, only D1-bound 13 nm AuNPs were mixed with the Origami-A. It is expected that there would be two AuNPs hybridized from their D1 to the two opposite sites of Origami-A, because D1 has free 3' end and it can only hybridize with one part of each site. Figure 5.4 shows that the NPs could be attached to the Origami. The constructed structure has two NPs with heights of more than 8 nm. Considering that the AuNPs have an average size 13 nm while synthesis, the measured size of 8 nm from the line analysis indicates that two of NPs are attached to each Origami as expected.

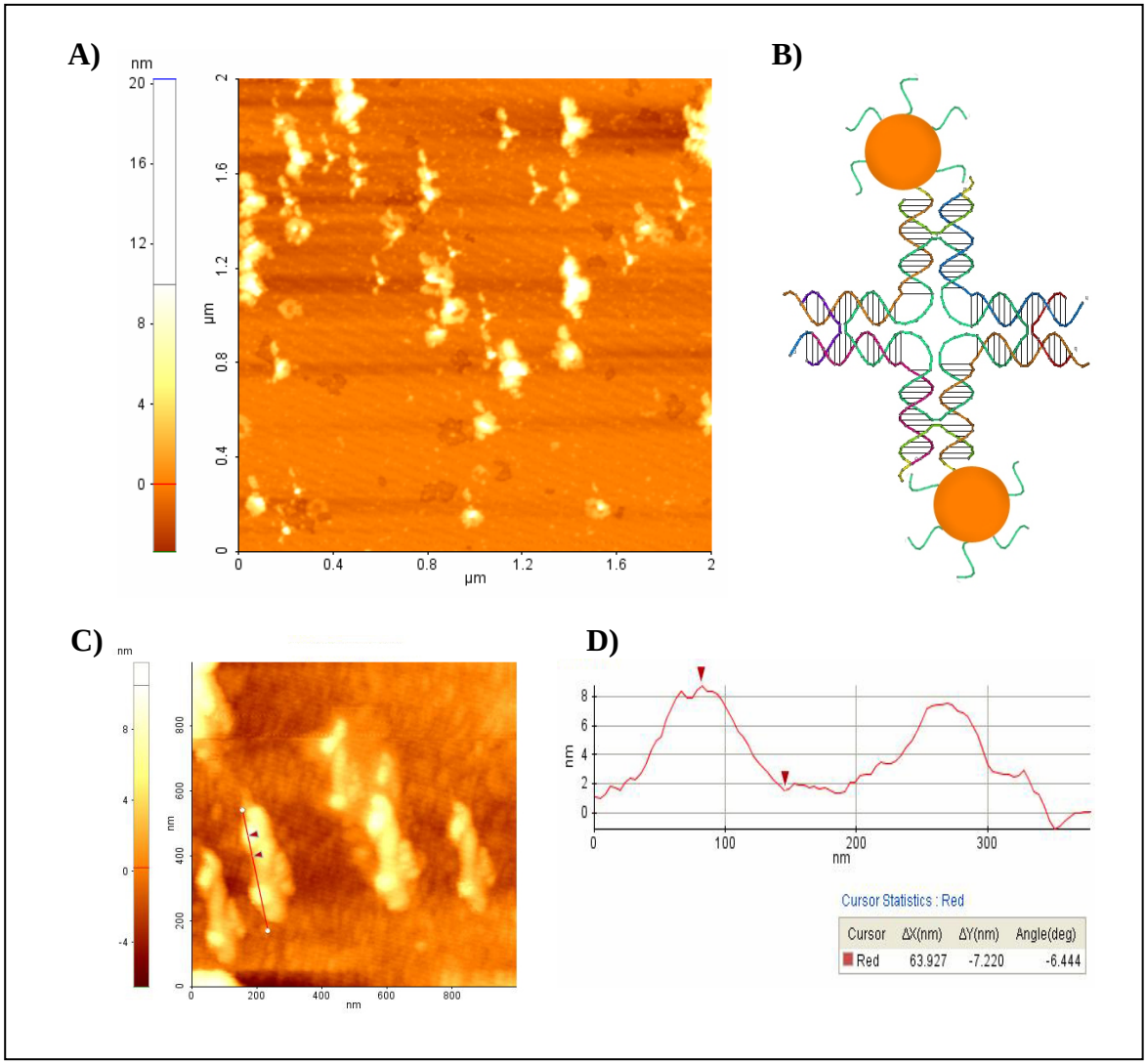

Figure 5.4. AFM images (A, C), schematic representation (B) and line analysis (D) of D1-bound AuNPs attached to Origami-A

5.1.2.4. D1-Bound and D2-Bound AuNPs Attached to Origami-A

The next step is to investigate whether both AuNPs can be attached to both sites of the Origami or not. In Figure 5.5, it is seen that the constructed nanostructures have more resemblance to its schematic representation, possibly, due to the fact that the rigidity of the structure increased after AuNPs were attached. Two 13 nm heighted AuNPs in one site can be clearly distinguished from line analysis. Additionally, the distance between AuNPs from opposite sites are measured as approximately 100 nm which also gives us a clue about the size of one Origami structure attached with AuNPs from both sites.

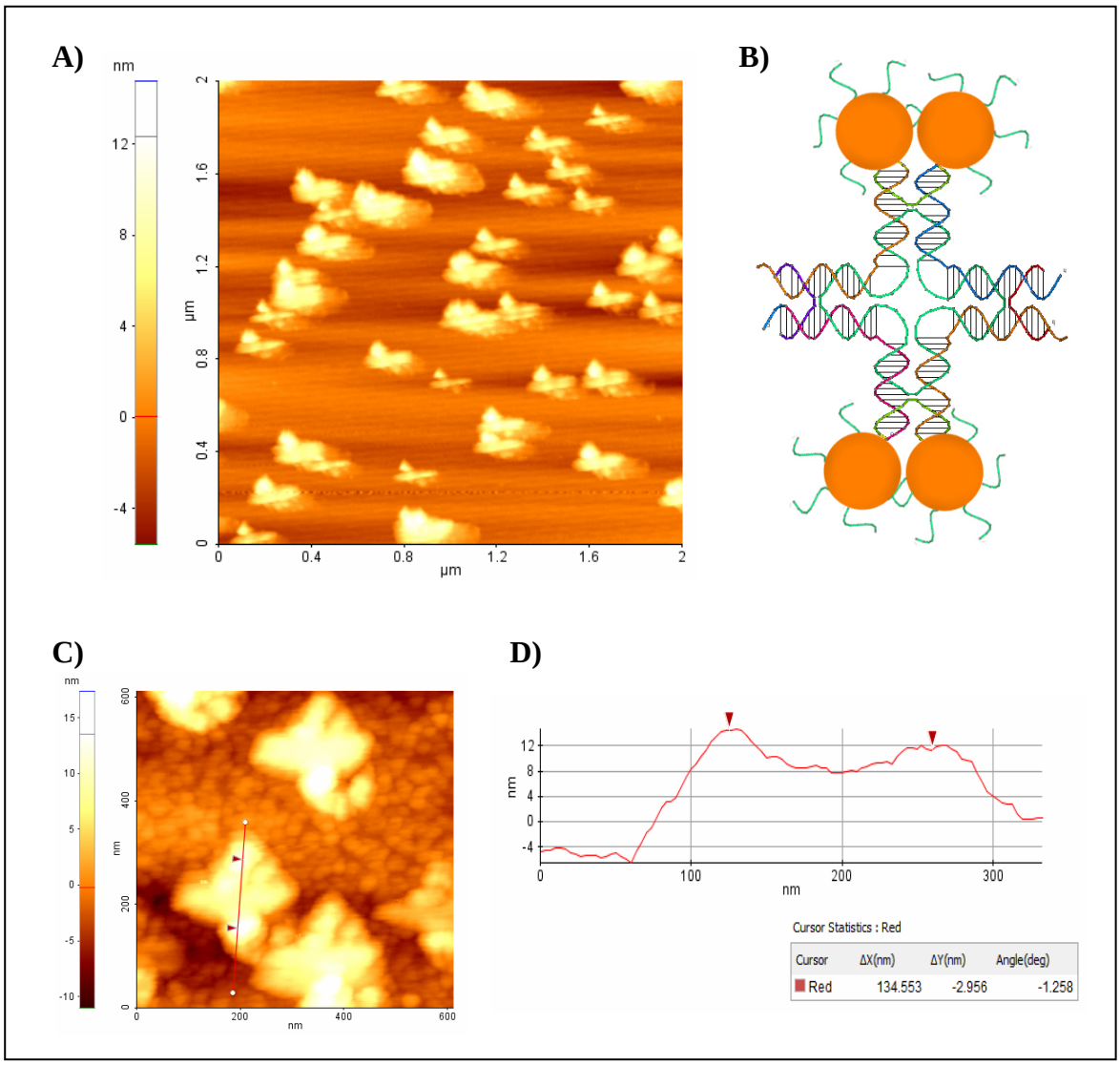

Figure 5.5. AFM images (A, C), schematic representation (B) and line analysis (D) of D1-bound or D2-bound AuNPs attached to Origami-A

5.1.2.5. D1-Bound AuNPs Attached to Mixture of Origami-A and Origami-B

In order to clarify that there is no hindrance for hybridization of AuNPs modified with ssDNA to the DNA Origami mixture, D1-bound AuNPs were mixed with the Origami-A and B mixture. The AFM image in Figure 5.5 shows that 13 nm AuNPs can be attached to the Origami mixture composed of three DNA Origami with a length of more than 200 nm. In the line analysis, the AuNPs are observed wide apart with a distance of 25 nm which is consistent with the size of one Origami.

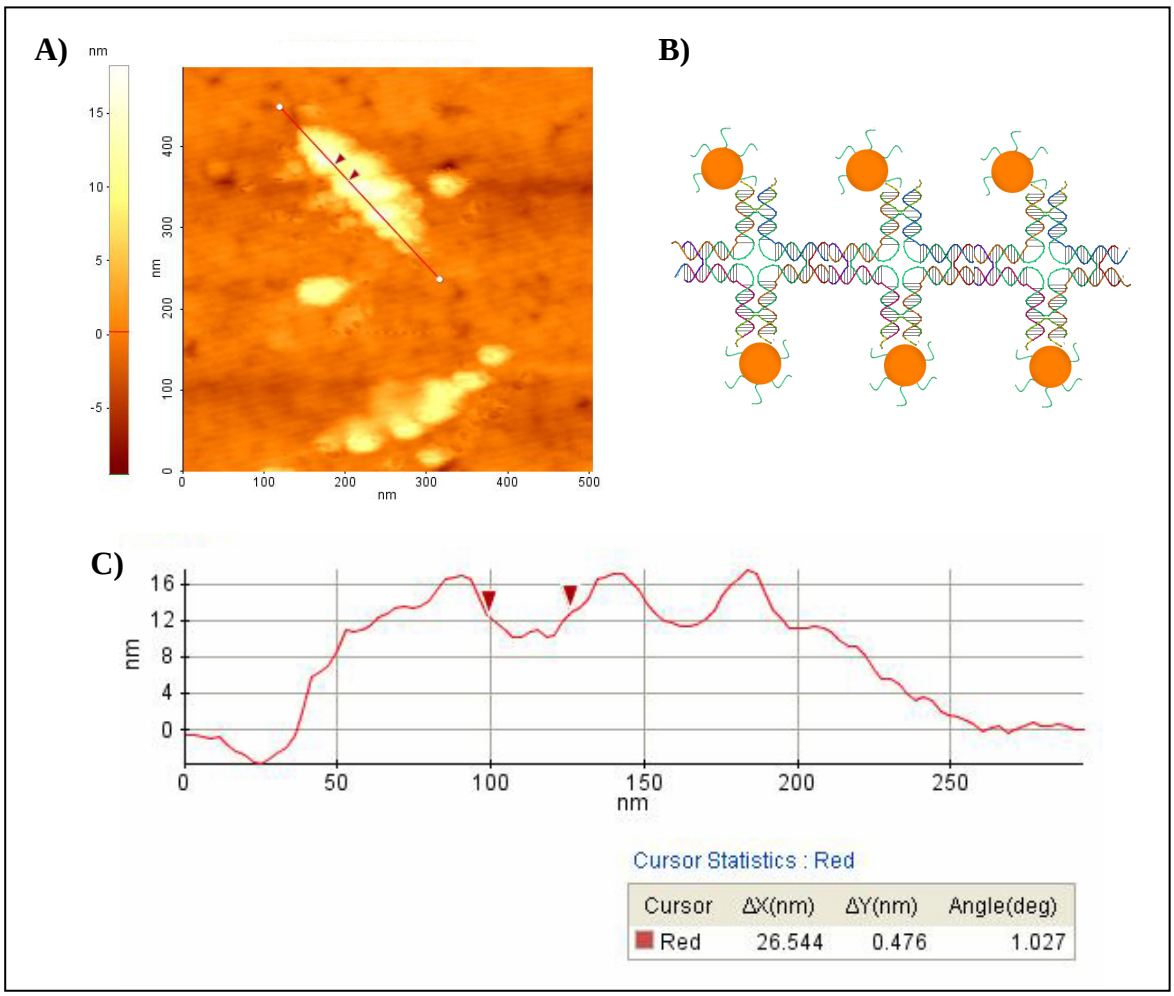

Figure 5.6. AFM image (A), schematic representation (B) and line analysis (C) of D1-bound AuNPs attached to the mixture of Origami-A and Origami-B

5.1.2.6. D1-Bound and D2-Bound AuNPs Attached to Mixture of OrA and OrB

Finally, both D1-bound and D2-bound 13 nm AuNPs were mixed with the mixture of Origami-A and Origami-B. Similar to previous step, interestingly, only three DNA Origami were hybridized with each other and the AuNPs were attached to them as seen in the AFM image in Figure 5.7. From line analysis of the AFM image, it is observed that the two AuNPs can be attached to the same site of the each Origami and the final structure seems to be constructed as 240 nm in length.

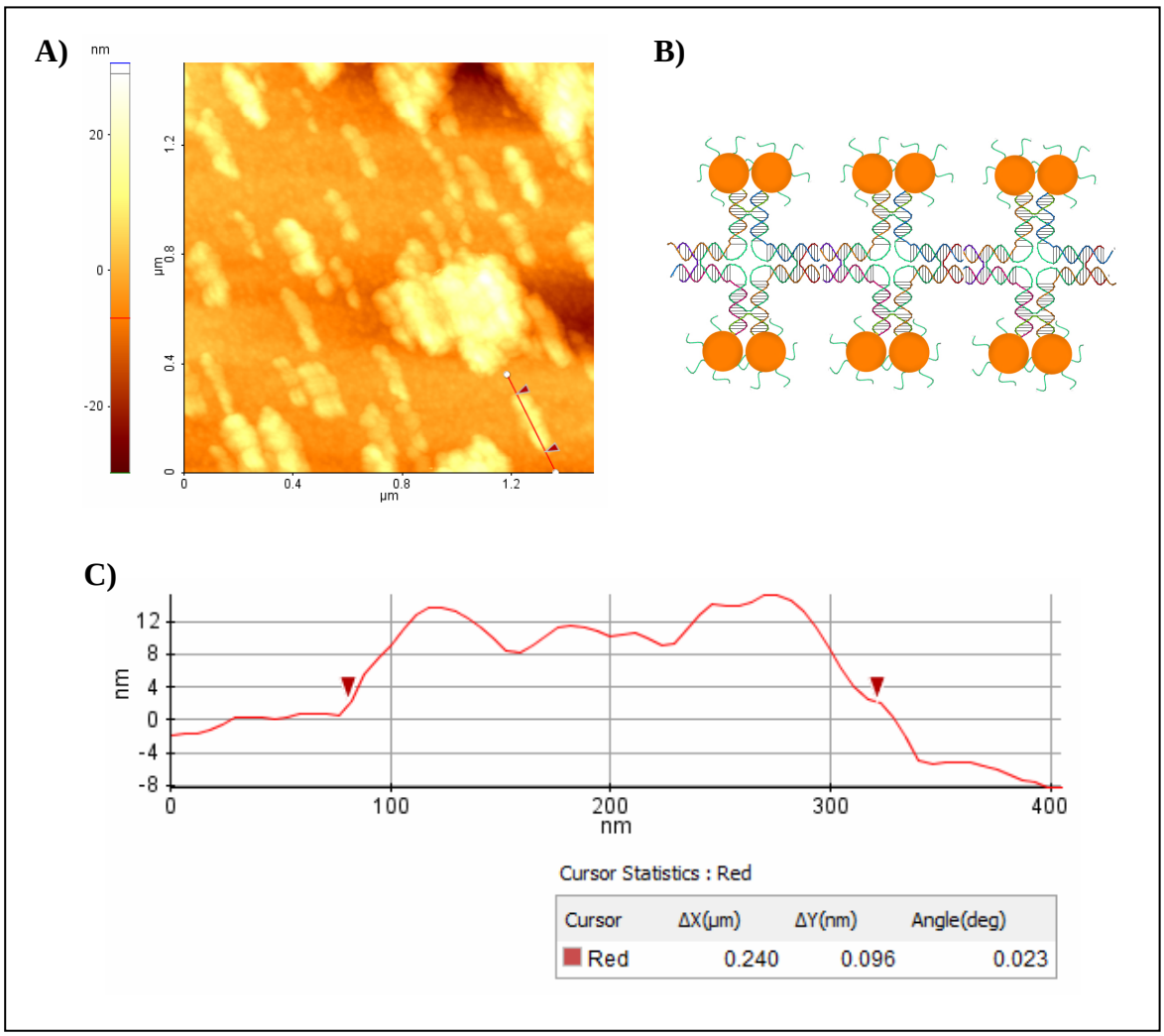

Figure 5.7. AFM image (A), schematic representation (B) and line analysis (C) of D1-bound or D2-bound AuNPs attached to the mixture of Origami-A and Origami-B

5.2. CONSTRUCTING NANOSTRUCTURES BY ADDING DNA LINKER

In the second part of the thesis, it is aimed to construct network formation which is made of AuNPs separated with a certain distance by adding DNA linkers with different sizes. The importance of generating such structures is realized in many application areas of science and technology such as in imaging and therapy in medicine. For this purpose, after 13 nm AuNPs were bound by D14 and D15 individually, one of the DNA linker from D16 to D25 was added to the mixture of their suspension which had equal number from both types of ODN-bound AuNPs as seen in Figure 5.8.

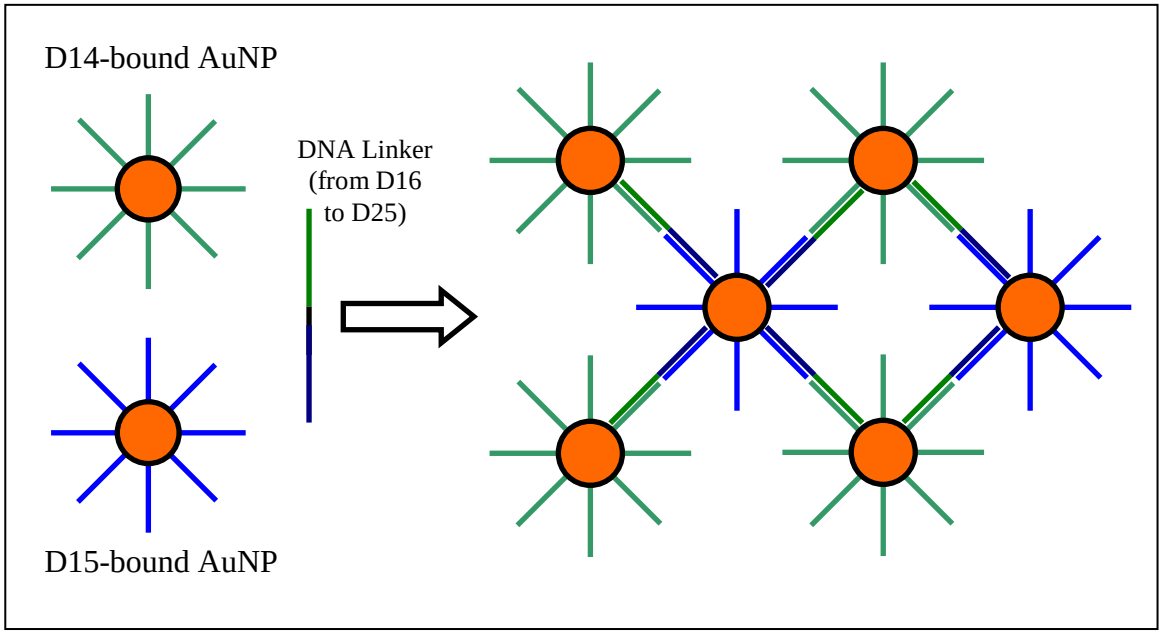

Figure 5.8. Schematic representation of nanostructure formation after DNA linker is added to two different ODN-bound 13 nm AuNPs

5.2.1. UV/Vis Spectroscopy Analysis

The mixture, firstly, was analyzed with UV/Vis Spectroscopy. The UV/Vis spectra of AuNPs give the maximum value according to the excitation wavelength of their surface plasmons. This maximum absorption depends on the size of the molecule bound to surface of the NPs and depends on how this molecule effects the electron configuration of the AuNPs. Figure 5.9 shows that AuNPs-alone, ODN-bound AuNPs and their mixtures give

maximum absorption at 523 nm; whereas the addition of DNA linker slightly shifts the maximum absorptions to 525 nm. This 2 nm shift may indicate that there is an interaction between AuNPs, however, it is difficult to say that this directly stems from the network formation of AuNPs.

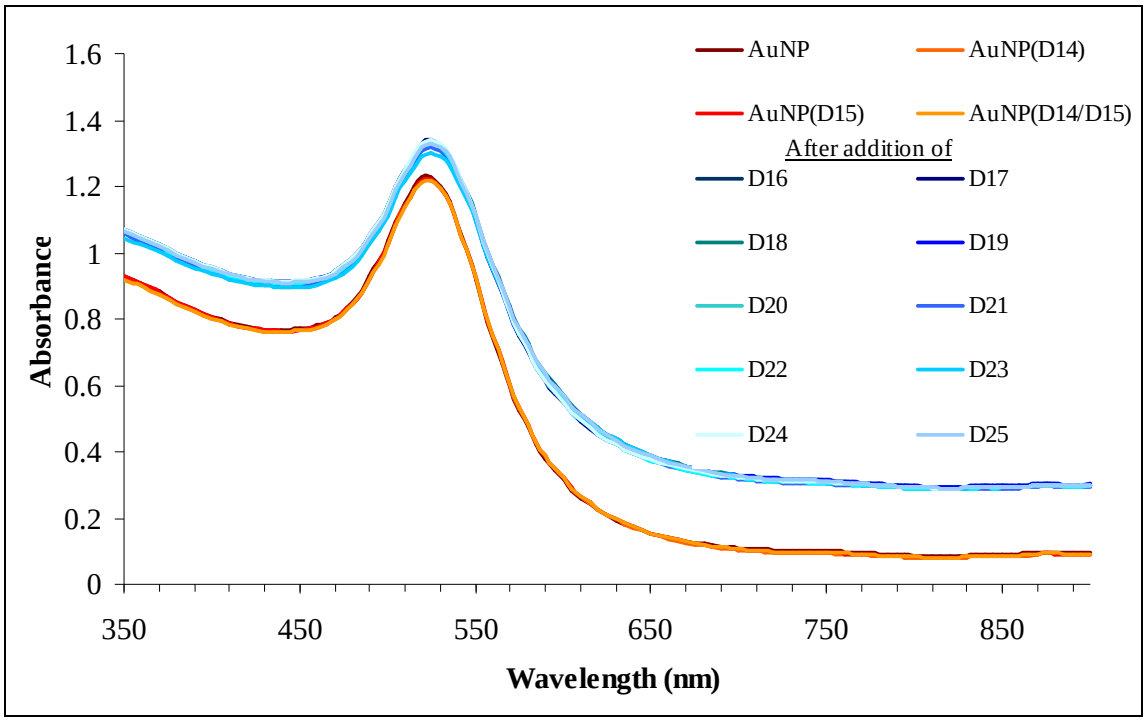

Figure 5.9. UV/Vis Spectroscopic graph of the AuNPs and nanostructures made of them by adding DNA linkers

5.2.2. Dynamic Light Scattering Analysis

In order to investigate whether the 2 nm shift of maximum absorption value in UV/Vis Spectroscopy was due to the attachment of the molecules on the AuNPs, DLS analysis was needed. DLS experiments, done by Zetasizer, provide clear information about the size of the materials in the suspension. In Figure 5.10, it is seen that the average size of ODN-bound AuNPs is measured as 24 nm and does not change after mixing of D14-bound and D15-bound AuNPs suspensions before DNA linkers are added. On the other hand, the average diameter of the structures present in the suspension increases to values between 120 nm to 200 nm after DNA linkers are added despite the fact that some of AuNPs remain free in suspension. From this result, it can be concluded that the DNA linkers assemble the

certain amount of AuNPs but not the all of them. This situation stems from that some of AuNPs did not contribute to the network formation due to the fact that the contributed AuNPs may be assembled in other crystalline forms in which building blocks are placed with different ratios rather than one to one. When the plot is redrawn by number distribution, however, the % number of free NPs dominates the % number of constructed structures as seen in Figure 5.11. However this does not mean that most of the NPs remain free, because it shows the number of structures formed, not related with the number of NPs present in the structures. The other question that may arise is why a size increase of 200 nm corresponds to a small, 2 nm, maximum absorption shift. It is known that the aggregation of AuNPs shifts the maximum absorption up to 550 nm due to overlapping of surface plasmons of the NPs. The answer is that although the NPs were assembled by DNA linkers; since the distances between the two AuNPs were kept by DNA in between and AuNPs were too far away from each other for overlapping of surface plasmons, the maximum absorption wavelength was not shifted to longer wavelengths as seen Figure 5.9.

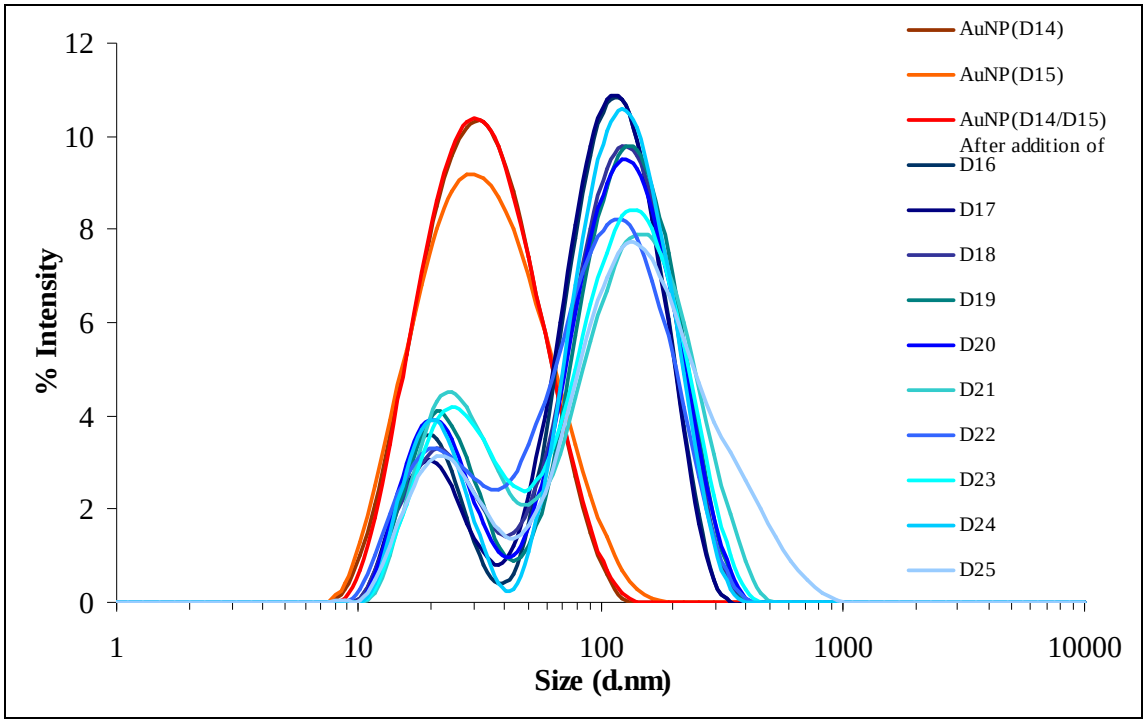

Figure 5.10. DLS analysis, distributed by % intensity, of the ODN-bound AuNPs and nanostructures made of them by adding DNA linkers

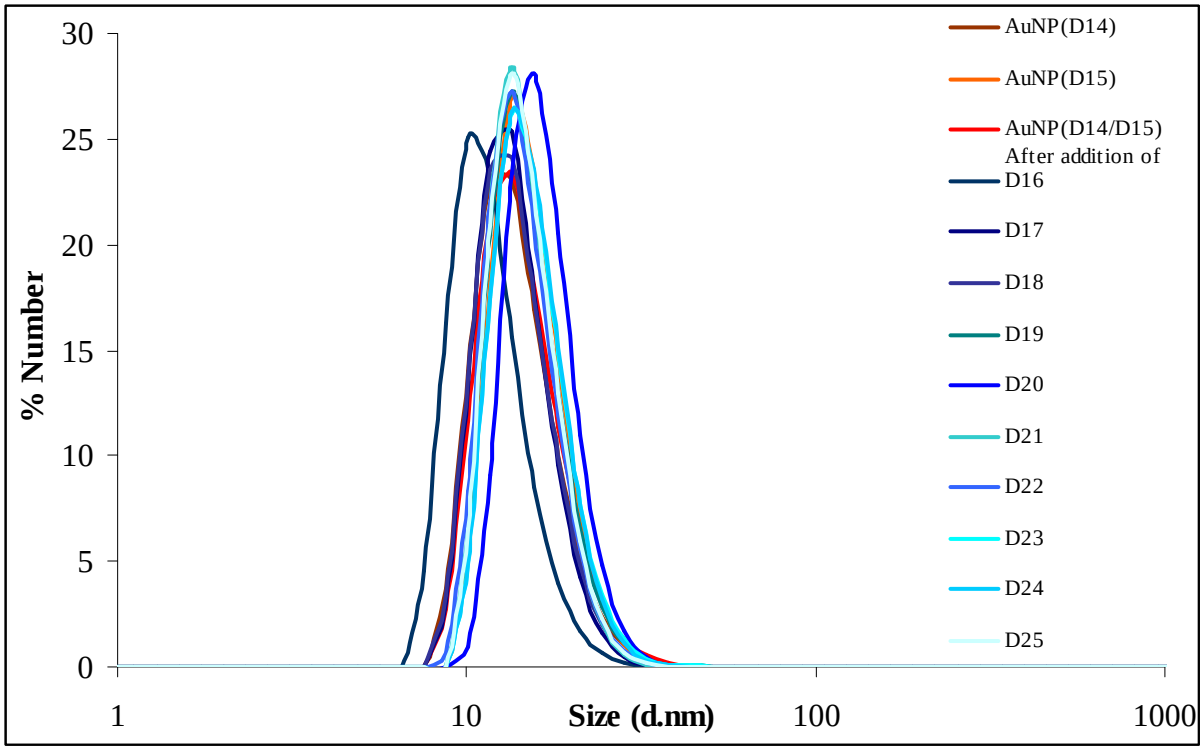

Figure 5.11. DLS analysis, distributed by % number, of the ODN-bound AuNPs and nanostructures made of them by adding DNA linkers

5.2.3. Small Angle X-Ray Scattering Analysis

The NPs have different behaviors in the suspension from that of on the surface. Though UV/Vis Spectroscopy and DLS give data about the size of the structures in the suspension, these techniques do not provide information about crystal form of the structure. Small Angle X-Ray Scattering (SAXS), however, explains whether the constructed structure is in crystalline form or amorphous form. Therefore, some of the prepared samples were analyzed with SAXS. Firstly, only ODN-bound AuNPs were analyzed to see whether they form any crystal. As seen in Figure 5.12 (A), D14 or D15-bound AuNPs have maximum scattered intensities as 5778 and 5719 respectively at the same magnitude of the scattering vector (q) 0.0158 $Å^{-1}$. Additionally, the curves have smooth lines, which mean that there is no crystalline formation in these suspensions, at higher q values. As far as after addition of a DNA linker is considered, there are notches on the curve that has maximum scattered intensity at 0.000791 $Å^{-1}$, seen in Figure 5.12 (B). These peaks at higher q values indicate that there are crystalline formations in the

suspension. The radius of gyration was calculated as 70.38 nm assuming the construct was globular and as 35.14 nm if the construct was assumed to have rod shape. The exact shape of the structure can only be decided after approximation to the pre-defined model shapes.

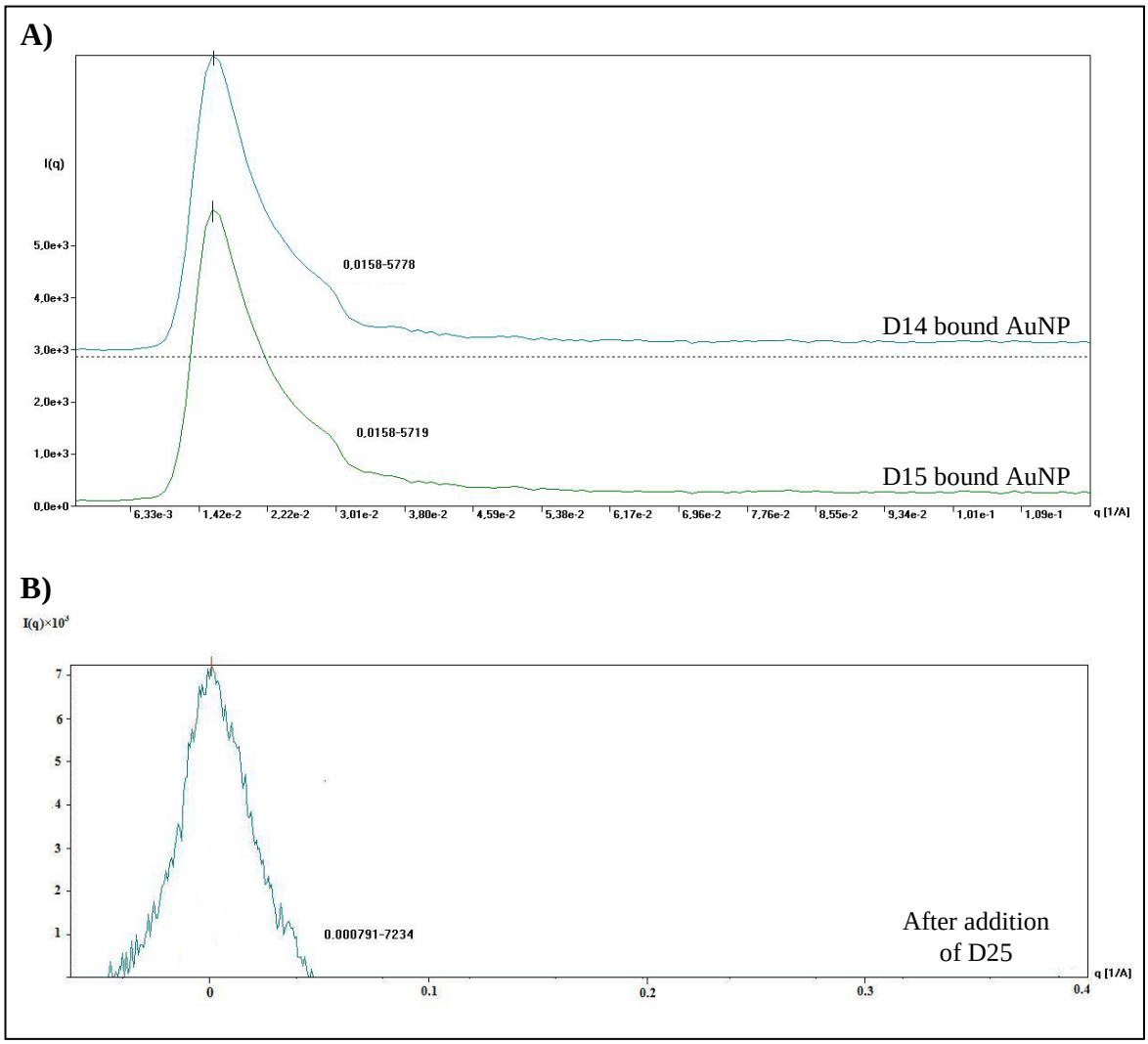

Figure 5.12. SAXS analysis of the ODN-bound AuNPs (A) and nanostructures after addition of DNA linker D25 (B)

To understand the properties of nanocubic structures formed in the suspension, further analysis were done. Nanostructures formed by D16 and D25 were selected to understand also the effect of distance between NPs on the crystalline formation. As seen in Figure 5.13, while there are four cubic parameters with the addition of D16, there are eight cubic parameters seen with the addition of D25. From this, it is concluded that more cubic

structures were formed in the latter one than in the former one. The spaces between lattices were measured to be larger in the constructed structure by addition of D25 than that of D16 as expected: 67.64 nm and 58.87 nm respectively.

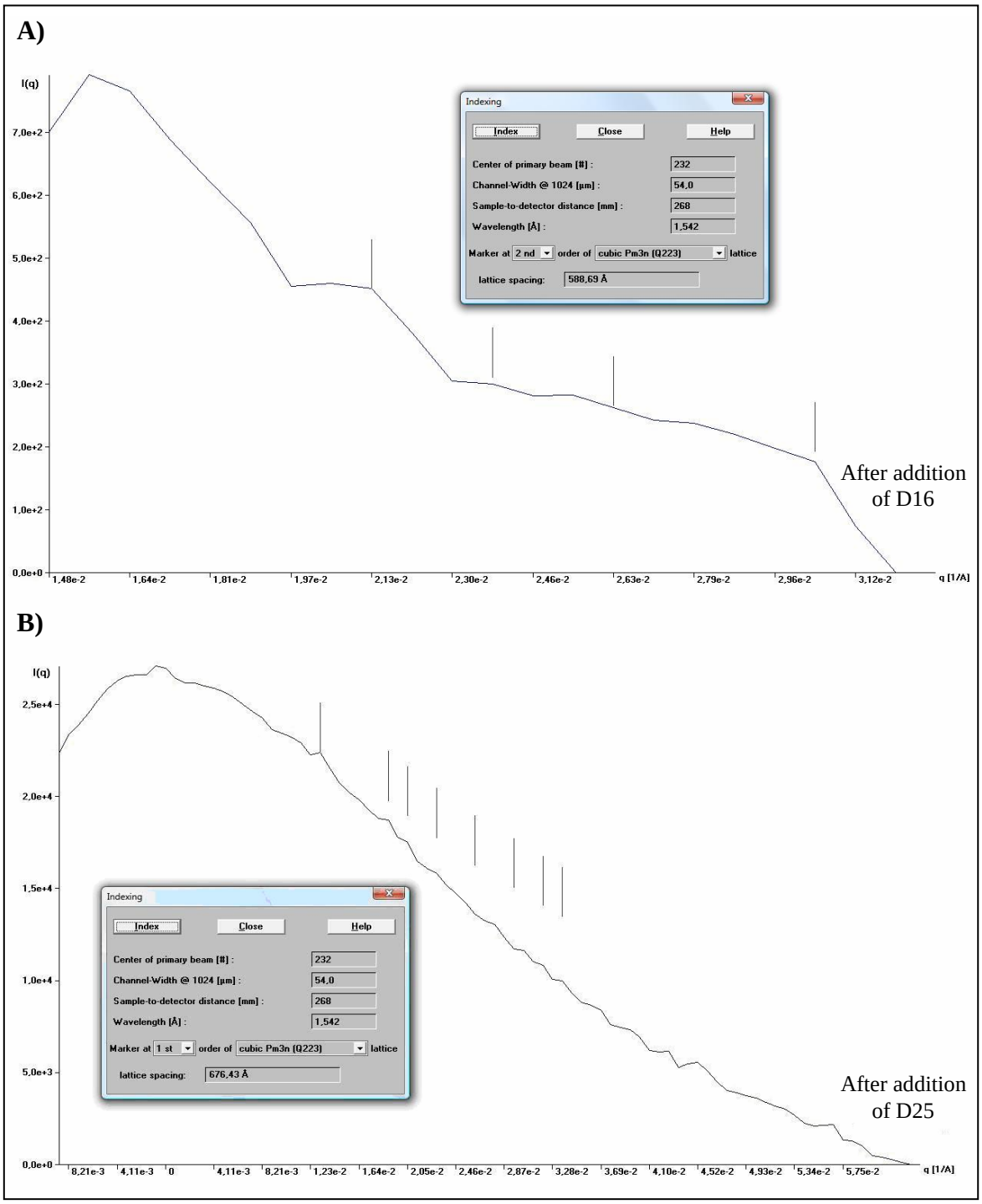

Figure 5.13. SAXS analysis of nanoconstructs by adding D16 (A) and D26 (B)

6. CONCLUSION AND RECOMMENDATIONS

6.1. CONCLUSION

Nanoconstructs provide special and unique properties. In this thesis, it is aimed to construct two different nanostructures in two different ways. In the first study, assembly of the 13 nm AuNPs into desired shape by using DNA Origami is investigated. The DNA Origami is constructed and elongation is realized by hybridization from the sticky ends of two Origami. Then it is shown that the AuNPs can be assembled on these DNA Origami structures which are used as a 2D template.

The second study includes the formation of cubic structures in nano scale. From the UV/Vis spectroscopy and DLS results, it is concluded that it is also possible to produce network formation by adding DNA linkers to the mixture of ODN-bound AuNPs. The crystalline formation is found from SAXS analysis, which gives us information about nanocubic structures that are formed after addition of the DNA linkers. A construction of cubic structure in nanoscale is rather exciting information because of their unique properties. Additionally, higher distances and being unpaired part between AuNPs seems more helpful to nanocubic structures because of less hindrance and more flexibility.

In conclusion, new nanoconstructs are produced in this work. This thesis outlines and clarifies each step in the construction of nanostructures for the design and preparation of higher structures using the NPs as building blocks.

6.2. RECOMMENDATIONS

In the future work of this thesis, the construction of novel structures should be pursued. The first part of the study, especially, shows that it is possible to fabricate nanodevices and nanomachines from metal nanoparticles. After construction of DNA Origami structure with a definite shape and assembling of nanoparticles on it, it is possible and easy to fabricate high throughput nanostructures. Besides their smallness, they would work more efficient compared to their macro examples due to quantum effect. With the results of this study, nanomotors, nanoplanes and even nano washing machines etc. would not be a dream in the future. These nanodevices and nanomachines can be used in medicine, military and in any public interests.

The second part of the thesis open minds to use nanocubic structures in temperature sensitive applications. Mixing of two ODN-bound NPs in different ratios, especially 3:4 and 1:8, would force the assembly of NPs into face-centered or body-centered cubic forms. Depends on the centered NPs, these structures can be used in different purposes. For instance, Quantum Dots can be centered and gold nanoparticles can be placed at the corners, and after heating up, since the DNAs are unhybridized, the QDs would be free to be used in imaging systems. Additionally, this temperature-sensitive imaging system would be more biocompatible because toxic QDs are hidden in the cubic structure and only be free if the temperature increases to a certain degree. Moreover, having silver nanoparticles as the center nanoparticle of the cubic face provides useful contribution in plasmonic studies such as surface-enhanced Raman spectroscopy.

Based on the principles of nanoconstruction presented in this thesis, near and far future directions in the development of nanoscience will be widened.

REFERENCES

1. Faraday, M., “The Bakerian Lecture: Experimental Relations of Gold (and Other Metals) to Light”, Philosophical Transactions of the Royal Society of London, No. 147, pp. 145-181, 1857.

2. Feynman, R. P., “There's plenty of room at the bottom”, Engineering and Science, Vol. 23, No. 5, pp. 22-36, 1960.

3. Taniguchi, N., On the Basic Concept of Nanotechnology, Proceedings of the International Conference on Production Engineering, Tokyo, 1974.

4. Freestone, I., N. Meeks, M. Sax and C. Higgitt, "The Lycurgus Cup - A Roman nanotechnology", Gold Bulletin, Vol. 40, No. 4, pp. 270-277, 2007.

5. Schultz, W., "Crafting a National Nanotechnology Effort", Chemical and Engineering News, Vol. 78, No. 42, pp. 39–42, 2000.

6. Kawasaki, E. S. and A. Player, "Nanotechnology, nanomedicine, and the development of new, effective therapies for cancer", Nanomedicine, Vol. 1, No. 2, pp. 101-109, 2005.

7. Wolf, E. L., Nanophysics and Nanotechnology: An Introduction to Modern Concepts in Nanoscience, Wiley-VCH, Weinheim, 2004.

8. Lubick, N., "Silver socks have cloudy lining", Environmental Science & Technology, Vol. 42, No. 11, pp. 3910-3910, 2008.

9. Wang, X., J. Zhuang, Q. Peng and Y. D. Li, "A general strategy for nanocrystal synthesis", Nature, Vol. 437, No. 7055, pp. 121-124, 2005.

10. Murray, C. B., D. J. Norris and M. G. Bawendi, "Synthesis and Characterization of Nearly Monodisperse Cde (E = S, Se, Te) Semiconductor Nanocrystallites", Journal of the American Chemical Society, Vol. 115, No. 19, pp. 8706-8715, 1993.

11. Yin, Y. and A. P. Alivisatos, "Colloidal nanocrystal synthesis and the organic-inorganic interface", Nature, Vol. 437, No. 7059, pp. 664-670, 2005.

12. Pileni, M. P., "Nanocrystal self-assemblies: Fabrication and collective properties", Journal of Physical Chemistry B, Vol. 105, No. 17, pp. 3358-3371, 2001.

13. Lee, P. C. and D. Meisel, "Adsorption and Surface-Enhanced Raman of Dyes on Silver and Gold Sols", Journal of Physical Chemistry, Vol. 86, No. 17, pp. 3391-3395, 1982.

14. Madou, M. J., Fundamentals of Microfabrication, CRC, Boca Raton, 1997.

15. Dentinger, P. M., K. L. Krafcik, K. L. Simison, R. P. Janek and J. Hachman, "High aspect ratio patterning with a proximity ultraviolet source", Microelectronic Engineering, Vol. 61-2, No. pp. 1001-1007, 2002.

16. Yamazaki, K. and H. Namatsu, "Two-axis-of-rotation drive system in electron-beam lithography apparatus for nanotechnology applications", Microelectronic Engineering, Vol. 73-74, No. pp. 85-89, 2004.

17. Van Kan, J. A., A. A. Bettiol, K. Ansari, E. J. Teo, T. C. Sum and F. Watt, "Proton beam writing: a progress review", International Journal of Nanotechnology, Vol. 1, No. 4, pp. 464-479, 2004.

18. Achenbach, S., "Deep sub micron high aspect ratio polymer structures produced by hard X-ray lithography", Microsystem Technologies-Micro-and Nanosystems-Information Storage and Processing Systems, Vol. 10, No. 6-7, pp. 493-497, 2004.

19. Mirkin, C. A. and Niemeyer, C. M. (editors), Nanobiotechnology II, Wiley-VCH, Weinheim, 2007.

20. Dresselhaus, G. and P. Avouris, Carbon Nanotubes: Synthesis, Structure, Properties,and Applications, Springer, New York, 2001.

21. Saito, R. and M. S. Dresselhaus, Physical Properties of Carbon Nanotubes, Imperial College Press, London, 1998.

22. Meyyappan, M. (editor), Carbon Nanotubes Science and Applications, CRC Press, California, 2005.

23. Reich, S., C. Thomsen. and J. Maultzsch, Carbon Nanotubes: Basic Concepts and Physical Properties, Wiley-VCH, Berlin, 2004.

24. Kawasaki, E. S. and T. A. Player, “Nanotechnology, Nanomedicine, and the Development of New, Effective Therapies for Cancer”, Nanomedicine: Nanotechnology, Biology, and Medicine, Vol. 1, No. 2, pp. 101-109, 2005.

25. Hampton, T., “Researchers Use Dots to Light Up Tumor Cells”, Journal of the American Medical Association, Vol. 292, No. 16, pp. 1944-1945, 2004.

26. Salgueirino-Maceira, V., M. A. Correa-Duarte, M. Farle, A. Lopez-Quintela, K. Sieradzki and R. Diaz, "Bifunctional gold-coated magnetic silica spheres", Chemistry of Materials, Vol. 18, No. 11, pp. 2701-2706, 2006.

27. Lu, A. H., E. L. Salabas and F. Schuth, "Magnetic nanoparticles: Synthesis, protection, functionalization, and application", Angewandte Chemie-International Edition, Vol. 46, No. 8, pp. 1222-1244, 2007.

28. Frankamp, B. L., N. O. Fischer, R. Hong, S. Srivastava and V. M. Rotello, "Surface modification using cubic silsesquioxane ligands. Facile synthesis of water-soluble

metal oxide nanoparticles", Chemistry of Materials, Vol. 18, No. 4, pp. 956-959, 2006.

29. Kahraman, M., M. M. Yazici, F. Sahin, O. F. Bayrak and M. Culha, "Reproducible surface-enhanced Raman scattering spectra of bacteria on aggregated silver nanoparticles", Applied Spectroscopy, Vol. 61, No. 5, pp. 479-485, 2007.

30. Cam, D., K. Keseroglu, M. Kahraman, F. Sahin and M. Culha, "Multiplex identification of bacteria in bacterial mixtures with surface-enhanced Raman scattering", Journal of Raman Spectroscopy, Vol. 41, No. 5, pp. 484-489, 2010.

31. Culha, M., M. Kahraman, D. Cam, I. Sayin and K. Keseroglu, “Rapid Identification of Bacteria and Yeast Using Surface-Enhanced Raman Scattering”, Surface and Interface Analysis, Vol. 42, No. 6-7, pp. 462-465, 2009.

32. Chen, C. Y. and C. L. Chiang, “Preparation of Cotton Fibers with Antibacterial Silver Nanoparticles”, Materials Letters, Vol. 62, No. 21, pp. 3607-3609, 2008.

33. Sondi, I. and B. Salopek-Sondi, "Silver nanoparticles as antimicrobial agent: a case study on E-coli as a model for Gram-negative bacteria", Journal of Colloid and Interface Science, Vol. 275, No. 1, pp. 177-182, 2004.

34. Huang, X. H., I. H. El-Sayed, W. Qian and M. A. El-Sayed, "Cancer cell imaging and photothermal therapy in the near-infrared region by using gold nanorods", Journal of the American Chemical Society, Vol. 128, No. 6, pp. 2115-2120, 2006.

35. Everts, M., V. Saini, J. L. Leddon, R. J. Kok, M. Stoff-Khalili, M. A. Preuss, C. L. Millican, G. Perkins, J. M. Brown, H. Bagaria, D. E. Nikles, D. T. Johnson, V. P. Zharov and D. T. Curiel, "Covalently linked au nanoparticles to a viral vector: Potential for combined photothermal and gene cancer therapy", Nano Letters, Vol. 6, No. 4, pp. 587-591, 2006.

36. Gibson, J. D., B. P. Khanal and E. R. Zubarev, "Paclitaxel-functionalized gold nanoparticles", Journal of the American Chemical Society, Vol. 129, No. 37, pp. 11653-11661, 2007.

37. Seydel, C., "Quantum dots get wet", Science, Vol. 300, No. 5616, pp. 80-81, 2003.

38. Baughman, R. H., A. A. Zakhidov and W. A. de Heer, "Carbon nanotubes - the route toward applications", Science, Vol. 297, No. 5582, pp. 787-792, 2002.

39. Pankhurst, Q. A., J. Connolly, S. K. Jones and J. Dobson, "Applications of magnetic nanoparticles in biomedicine", Journal of Physics D-Applied Physics, Vol. 36, No. 13, pp. R167-R181, 2003.

40. I. Sayin, I., M. Kahraman, F. Sahin, D. Yurdakul and M. Culha, "Characterization of Yeast Species Using Surface-Enhanced Raman Scattering", Applied Spectroscopy, Vol. 63, No. 11, pp. 1276-1282, 2009.

41. Sardar, R., A. M. Funston, P. Mulvaney and R. W. Murray, "Gold Nanoparticles: Past, Present, and Future", Langmuir, Vol. 25, No. 24, pp. 13840-13851, 2009.

42. Credi, A., Nanotecnologia Molecolare: Introduction, http://www.ciam.unibo.it/photochem/MNano01.pdf, 2007

43. Pang, J. B., S. S. Xiong, F. Jaeckel, Z. C. Sun, D. Dunphy and C. J. Brinker, "Free-standing, patternable nanoparticle/polymer monolayer arrays formed by evaporation induced self-assembly at a fluid interface", Journal of the American Chemical Society, Vol. 130, No. 11, pp. 3284-3285, 2008.

44. Binder, W. H., "Supramolecular assembly of nanoparticles at liquid-liquid interfaces", Angew Chem Int Ed Engl, Vol. 44, No. 33, pp. 5172-5175, 2005.

45. Boker, A., Y. Lin, K. Chiapperini, R. Horowitz, M. Thompson, V. Carreon, T. Xu, C. Abetz, H. Skaff, A. D. Dinsmore, T. Emrick and T. P. Russell, "Hierarchical

nanoparticle assemblies formed by decorating breath figures", Nat Mater, Vol. 3, No. 5, pp. 302-306, 2004.

46. Gu, H. W., Z. M. Yang, J. H. Gao, C. K. Chang and B. Xu, "Heterodimers of nanoparticles: Formation at a liquid-liquid interface and particle-specific surface modification by functional molecules", Journal of the American Chemical Society, Vol. 127, No. 1, pp. 34-35, 2005.

47. Binks, B. P. and J. H. Clint, "Solid wettability from surface energy components: Relevance to pickering emulsions", Langmuir, Vol. 18, No. 4, pp. 1270-1273, 2002.

48. Mizuno, M., Y. Sasaki, A. C. C. Yu and M. Inoue, "Prevention of nanoparticle coalescence under high-temperature annealing", Langmuir, Vol. 20, No. 26, pp. 11305-11307, 2004.

49. Demers, L. M., D. S. Ginger, S. J. Park, Z. Li, S. W. Chung and C. A. Mirkin, "Direct patterning of modified oligonucleotides on metals and insulators by dip-pen nanolithography", Science, Vol. 296, No. 5574, pp. 1836-1838, 2002.

50. Mulder, A., J. Huskens and D. N. Reinhoudt, "Multivalency in supramolecular chemistry and nanofabrication", Organic & Biomolecular Chemistry, Vol. 2, No. 23, pp. 3409-3424, 2004.

51. Boal, A. K., F. Ilhan, J. E. DeRouchey, T. Thurn-Albrecht, T. P. Russell and V. M. Rotello, "Self-assembly of nanoparticles into structured spherical and network aggregates", Nature, Vol. 404, No. 6779, pp. 746-748, 2000.

52. Sanyal, A., T. B. Norsten, O. Uzun and V. M. Rotello, "Adsorption/Desorption of mono- and diblock copolymers on surfaces using specific hydrogen bonding interactions", Langmuir, Vol. 20, No. 14, pp. 5958-5964, 2004.

53. Bigioni, T. P., X. M. Lin, T. T. Nguyen, E. I. Corwin, T. A. Witten and H. M. Jaeger, "Kinetically driven self assembly of highly ordered nanoparticle monolayers", Nature Materials, Vol. 5, No. 4, pp. 265-270, 2006.

54. Rabani, E., D. R. Reichman, P. L. Geissler and L. E. Brus, "Drying-mediated self-assembly of nanoparticles", Nature, Vol. 426, No. 6964, pp. 271-274, 2003.

55. Deegan, R. D., O. Bakajin, T. F. Dupont, G. Huber, S. R. Nagel and T. A. Witten, "Capillary flow as the cause of ring stains from dried liquid drops", Nature, Vol. 389, No. 6653, pp. 827-829, 1997.

56. Deegan, R. D., O. Bakajin, T. F. Dupont, G. Huber, S. R. Nagel and T. A. Witten, "Contact line deposits in an evaporating drop", Physical Review E, Vol. 62, No. 1, pp. 756-765, 2000.

57. Adachi, E., A. S. Dimitrov and K. Nagayama, "Stripe Patterns Formed on a Glass-Surface during Droplet Evaporation", Langmuir, Vol. 11, No. 4, pp. 1057-1060, 1995.

58. Shmuylovich, L., A. Q. Shen and H. A. Stone, "Surface morphology of drying latex films: Multiple ring formation", Langmuir, Vol. 18, No. 9, pp. 3441-3445, 2002.

59. Gates, B. D., Q. B. Xu, M. Stewart, D. Ryan, C. G. Willson and G. M. Whitesides, "New approaches to nanofabrication: Molding, printing, and other techniques", Chemical Reviews, Vol. 105, No. 4, pp. 1171-1196, 2005.

60. Cui, Y., M. T. Bjork, J. A. Liddle, C. Sonnichsen, B. Boussert and A. P. Alivisatos, "Integration of colloidal nanocrystals into lithographically patterned devices", Nano Letters, Vol. 4, No. 6, pp. 1093-1098, 2004.

61. Lehn, J. M., Supramolecular Chemistry: Concepts and Perspectives, John Wiley & Sons, New York, 1995.

62. Caruso, F., "Nanoengineering of particle surfaces", Advanced Materials, Vol. 13, No. 1, pp. 11-22, 2001.

63. Hamad-Schifferli, K., J. J. Schwartz, A. T. Santos, S. G. Zhang and J. M. Jacobson, "Remote electronic control of DNA hybridization through inductive coupling to an attached metal nanocrystal antenna", Nature, Vol. 415, No. 6868, pp. 152-155, 2002.

64. Chworos, A., I. Severcan, A. Y. Koyfman, P. Weinkam, E. Oroudjev, H. G. Hansma and L. Jaeger, "Building programmable jigsaw puzzles with RNA", Science, Vol. 306, No. 5704, pp. 2068-2072, 2004.

65. Vauthey, S., S. Santoso, H. Y. Gong, N. Watson and S. G. Zhang, "Molecular self-assembly of surfactant-like peptides to form nanotubes and nanovesicles", Proceedings of the National Academy of Sciences of the United States of America, Vol. 99, No. 8, pp. 5355-5360, 2002.

66. Schnur, J. M., "Lipid Tubules - a Paradigm for Molecularly Engineered Structures", Science, Vol. 262, No. 5140, pp. 1669-1676, 1993.

67. Lim, Y. B., S. Park, E. Lee, H. Jeong, J. H. Ryu, M. S. Lee and M. Lee, "Glycoconjugate nanoribbons from the self-assembly of carbohydrate-peptide block molecules for controllable bacterial cell cluster formation", Biomacromolecules, Vol. 8, No. 5, pp. 1404-1408, 2007.

68. Groger, G., V. Stepanenko, F. Wurthner and C. Schmuck, "Step-wise self-assembly of a small molecule with two orthogonal binding interactions leads to single stranded linear polymers in DMSO", Chemical Communications, No. 6, pp. 698-700, 2009.

69. Mirkin, C. A., R. L. Letsinger, R. C. Mucic and J. J. Storhoff, "A DNA-based method for rationally assembling nanoparticles into macroscopic materials", Nature, Vol. 382, No. 6592, pp. 607-609, 1996.

70. Mucic, R. C., J. J. Storhoff, C. A. Mirkin and R. L. Letsinger, "DNA-directed synthesis of binary nanoparticle network materials", Journal of the American Chemical Society, Vol. 120, No. 48, pp. 12674-12675, 1998.

71. Alivisatos, A. P., K. P. Johnsson, X. G. Peng, T. E. Wilson, C. J. Loweth, M. P. Bruchez and P. G. Schultz, "Organization of 'nanocrystal molecules' using DNA", Nature, Vol. 382, No. 6592, pp. 609-611, 1996.

72. Shih, W. M., J. D. Quispe and G. F. Joyce, "A 1.7-kilobase single-stranded DNA that folds into a nanoscale octahedron", Nature, Vol. 427, No. 6975, pp. 618-621, 2004.

73. Rothemund, P. W. K., "Folding DNA to create nanoscale shapes and patterns", Nature, Vol. 440, No. 7082, pp. 297-302, 2006.

74. Yan, H., S. H. Park, G. Finkelstein, J. H. Reif and T. H. LaBean, "DNA-templated self-assembly of protein arrays and highly conductive nanowires", Science, Vol. 301, No. 5641, pp. 1882-1884, 2003.

75. Andersen, E. S., M. Dong, M. M. Nielsen, K. Jahn, R. Subramani, W. Mamdouh, M. M. Golas, B. Sander, H. Stark, C. L. P. Oliveira, J. S. Pedersen, V. Birkedal, F. Besenbacher, K. V. Gothelf and J. Kjems, "Self-assembly of a nanoscale DNA box with a controllable lid", Nature, Vol. 459, No. 7243, pp. 73-75, 2009.

76. Sharma, J., R. Chhabra, A. Cheng, J. Brownell, Y. Liu and H. Yan, "Control of Self-Assembly of DNA Tubules Through Integration of Gold Nanoparticles", Science, Vol. 323, No. 5910, pp. 112-116, 2009.

77. Nykypanchuk, D., M. M. Maye, D. van der Lelie and O. Gang, "DNA-guided crystallization of colloidal nanoparticles", Nature, Vol. 451, No. 7178, pp. 549-552, 2008.

78. Park, S. Y., A. K. R. Lytton-Jean, B. Lee, S. Weigand, G. C. Schatz and C. A. Mirkin, "DNA-programmable nanoparticle crystallization", Nature, Vol. 451, No. 7178, pp. 553-556, 2008.

79. Hill, H. D., R. J. Macfarlane, A. J. Senesi, B. Lee, S. Y. Park and C. A. Mirkin, "Controlling the lattice parameters of gold nanoparticle FCC crystals with duplex DNA linkers", Nano Letters, Vol. 8, No. 8, pp. 2341-2344, 2008.

80. Macfarlane, R. J., B. Lee, H. D. Hill, A. J. Senesi, S. Seifert and C. A. Mirkin, "Assembly and organization processes in DNA-directed colloidal crystallization", Proceedings of the National Academy of Sciences of the United States of America, Vol. 106, No. 26, pp. 10493-10498, 2009.

81. Hill, H. D., J. E. Millstone, M. J. Banholzer and C. A. Mirkin, "The Role Radius of Curvature Plays in Thiolated Oligonucleotide Loading on Gold Nanoparticles", ACS Nano, Vol. 3, No. 2, pp. 418-424, 2009.